Republic of Iraq

Ministry of Higher Education & Scientific Research

University of Kerbala

College of Engineering

Mechanical Engineering Department

Using Magneto-Rheological (MR) Damper for Enhancement Vehicle Suspension System Response

A Thesis Submitted to the Council of the Faculty of the College of the Engineering/University Of Kerbala in Partial Fulfillment of the Requirements for the Master Degree in Mechanical Engineering (Applied Mechanics)

Written By:

Hussein Mohanned Hussein

(B.Sc. Mech. Eng. 2019)

Supervised By:

Assist. Prof. Dr. Ali Ibrahim Al-Zughaibi

Prof. Dr. Emad Qasem Hussein

February 2023   Rajab 1443

1

بسم الله الرحمن الرحيم

يَرْفَعِ اللَّهُ الَّذِينَ آمَنُوا مِنكُمْ وَالَّذِينَ أُوتُوا

الْعِلْمَ دَرَجَاتٍ

صدق الله العلي العظيم

(المجادلة: من الآية 11)
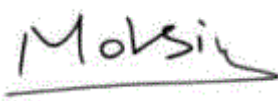
i

Examination committee certification

We certify that we have read the thesis entitled **"Using Magneto-Rheological (MR) Damper for Enhancement Vehicle Suspension System Response"** and as an examining committee, we examined the student "Hussein Mohanned Hussein" in its content and in what is connected with it and that in our opinion it is adequate as a thesis for the degree of Master of Science in Mechanical Engineering (Applied Mechanics).

Signature:

Name: Assist. Prof. Dr. Ali I. Al-Zughaibi

Date: /   / 2023

(Supervisor)

Signature:

Name: Prof. Dr. Emad Q. Hussein

Date: /   / 2023

(Supervisor)

Signature:

Name : Assist. Prof. Dr.Muslim M. Ali

Date: /   / 2023

(Member)

Signature:

Name :Lecturer. Dr. Ahmed Qassem

Date: /   / 2023

(Member)

Signature:

Name: Prof. Dr. Mohsin A AL-Shammari

Date: /   / 2023

(Chairman)

Signature :

Name : Assist. Prof. Dr.Hayder Jabber Kurji

Head of the Department of Mechanical Engineering

Date: /   / 2023

Signature:

Name : Prof. Dr.Laith Shakir Rasheed

Dean of the Engineering College

Date: /   / 2023

i

Supervisor certificate

We certify that the thesis entitled **"Using Magneto-Rheological (MR) Damper for Enhancement Vehicle Suspension System Response"** was prepared by Hussein Mohanned Hussein under our supervision at the Department of Mechanical Engineering, Faculty of Engineering, University of Kerbala as a partial of fulfilment of the requirements for the Degree of Master of Science in Mechanical Engineering.

Signature:

Assist. Prof. Dr. Ali Ibrahim Al-Zughaibi

Date: /   / 2023

Signature:

Prof. Dr. Emad Qasem Hussein

Date: /   / 2023

Linguistic certificate

I certify that the thesis entitled " Using Magneto-Rheological (MR) Damper for Enhancement Vehicle Suspension System Response " which has been submitted by has been proofread and its language has been amended to meet the English style.

Signature:

Linguistic advisor: Dr. Raheem S. Jamel

Date: / / 2023

Abstract

Suspension systems in vehicles are considered essential parts in the development of the automobile industry by increasing ride comfort and reliability in driving. In this thesis, the semi-active suspension system was studied and simulated using MR damper technology with the quarter-car model in simulating the system's response through the Matlab / Simulink environment. Magnetorheological (MR) dampers are adaptive devices whose properties can be adjusted through the application of a controlled voltage signal. A semi-active suspension system incorporating MR dampers combines the advantages of both active and passive suspensions. For this reason, there has been a continuous effort to develop control algorithms for MR-damped vehicle suspension systems to meet the requirements of the automotive industry. This thesis aims to investigate parametric techniques for identifying the nonlinear dynamics of an MR damper and Implement these techniques in the investigation of MR damper control of a vehicle suspension system that makes minimal use of sensors, thereby reducing the implementation cost and increasing system reliability. Four modern parametric models were selected, and a comparison was made in simulating the behaviour of the MR damper. The MR damper's non-linear behaviour is considered an essential obstacle in conducting an accurate simulation with the control systems that were used, namely (Skyhook with SFM). The modified Bouc-wen model is considered one of the most accurate models in the numerical simulation and is considered a stable model in explaining the hysteretic behaviour of the MR damper. The results showed a significant improvement in damping the vibrations resulting from the road profile by 50% and 39%, Approximately of the vertical displacement and the vertical acceleration compared to the passive suspension.

Undertaking

I certify that research work titled **"Magneto-Rheological (MR) Damper for Enhancement Vehicle Suspension System Response"** is my own work. The work has not been presented elsewhere for assessment. Where material has been used from other sources it has been properly acknowledged / referred.

Signature:

Hussein Mohanned Hussein

Date: /   / 2023

Acknowledgements

Table of Contents

List of Tables

List of Figures

List of Abbreviations

2DOF	Two degree of freedom

ASRE	Approximating sequence of riccati equation
CSC	Continuous State Control
ER	Electrorheological
HBC	High-bandwidth configuration
HSF	Heaviside Step Function
LQG	Linear-Quadratic-Gaussian
LBC	low-bandwidth configuration
MBWM	Modified Bouc–Wen model
MDM	Modified Dahl model
MLGM1	Modified LuGre model I
MLGM2	Modified LuGre model II
MRDs	Magnetorheological dampers
MRFs	Magnetorheological fluids
NN	Neural networks
QCM	Quarter-car model
RSM	Response surface methodology
RNN	Inverse recurrent neural network
SDRE	State dependent riccati equation
SBM	Simple Bingham model
SBWM	Simple Bouc–Wen model
SFM	Signum Function Method
PID	Proportional integral derivative

List of Symbols

Symbol	Description	Unit
A	Hysteresis constant	------
C_{post}	Post-yield damping	N.s/m
C_0	Viscous dashpot	N.s/m
c_{sky}	Skyhook control's damping constant	----
F_{mr}	Damping force for MR dampers	N
F_c	Frictional force	N
F_0	Accumulator force	N
$F(t)$	Damping force	N
f_c	Coulomb friction	N
F_d	Desired damping force	N
f_d	Desired damping force by skyhook control's	N
F_{mr}	Damping force for MR dampers	N
H	Heaviside periodic function	----
H	Magnetic field	T
K_w	Tyre stiffness	N/m
K_b	Spring stiffness	N/m
M_b	Sprung Mass (bady mass)	Kg
M_w	Un-sprung Mass	Kg
$sgn()$	Signum function	----
u	Intrinsic variable dependency on voltage	V
v	Applied voltage	V
v_i	Voltage supply by technique HSF	V
v_{sign}	Voltage supply by technique SFM	V

V_{max}	Maximum voltage	V
x_b	Body displacements	m
x_w	Tyre displacements	m
y	Internal displacement of the MR damper	m
Z_r	Road excitation	m
z	Evolutionary variable	----
σ	Stiffness parameter	----
α	Scaling factor	----
η	Reflects the response time	s
η_0	Positive velocity function	m/s
γ, β	Hysteresis loop	cm^{-2}
τ	Fluid's shear stress	Pa
τ_y	Yielding shear stress	Pa

Chapter One

Introduction

Chapter 1. Introduction

1.1 Introduction

The most important fundamental factor in the automotive industry at present is the design of a soft suspension system that provides good isolation between the tires and the vehicle body for comfortable and safe driving for passengers. The suspension system consists of many levers, dampers and springs that isolate the car from road turbulence. On the other hand, maintain continuous contact between the tires and the road. Figure (1-1) shows the typical Quarter-car model(QCM) suspension system. The damper is the most important part of the suspension system, which smooths the shock caused by the road profile. It lessens the likelihood of an unforeseen roadblock. The principle of operation of most dampers is to dissipate heat resulting from vibration in the environment. As for electromagnetic dampers, the working principle is different:" Here, a synchronous machine, induction machine, or DC motor is used to transform vibration energy into electricity, which is then stored in a condenser or battery for later use"[1].
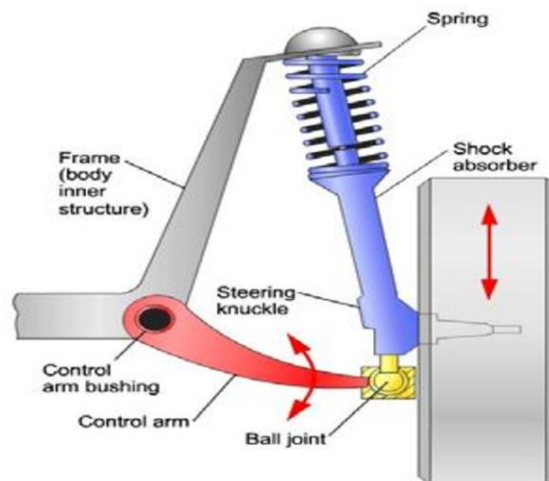
Figure 1-1: typical car suspension system

1.2 Classification of Vehicles suspension systems

Depending on how efficiently suspension systems can be controlled, they can be classified as passive, active, or semi-active. Although each sort of suspension system has its own set of advantages and problems.

1.2.1 Passive Suspension System

This kind of suspension is springs and oil dampers with consistent damping qualities make up passive suspension as shown in figure (1-2). in this model, The sprung mass and unsprung mass are represented by M_b and M_w, respectively, whereas K_b is the suspension stiffness constant and K_w is the tyre stiffness coefficient constant. C_b and C_w are the suspension and tyre damping constants, respectively; F_r is suspension friction; and Z_r, Z_w and Z_b are the road profile input, unsprung mass displacement, and sprung mass displacement, respectively[1].
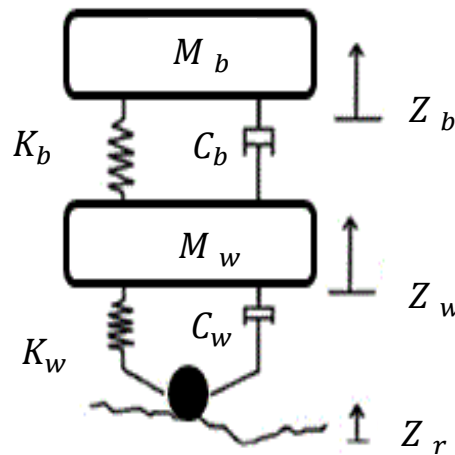
Figure 1-2 : Passive suspension system.

Passive suspension systems are often more straightforward, more dependable, and less expensive than active or semi-active suspension systems. The consistent damping characteristic is the primary problem with passive

suspension systems. For a passive suspension, softer springs and low to medium damping values are necessary, whereas hard springs and high damping values are needed to decrease the effects of dynamic forces. Designers utilize soft springs and a damper with low damping rates for applications that call for a comfortable and quiet ride, such as in a luxury car. Because the passive suspension system does not add energy to the system or require energy to perform its function, it is referred to as passive[2].

In a sports automobile, both stability, and control increase without sacrificing comfort by employing a stiff spring with a high damping rate damper. As a result, each area's performance is limited to the two opposing goals . Because the damper and spring properties of the passive suspension system cannot be modified according to the road profile, there is always a compromise to be made between ride handling and ride comfort.

1.2.2   Active Suspension System

The system of suspension in figure (1-3) show that the linkages are activated by expanding or compressing them as needed with the use of an active source of power. The traditional designs of automobile suspensions have been a balance between the three opposing parameters of road handling, suspension trip, and passenger comfort. In past years, car manufacturers have been able to satisfy all three necessary criteria independently thanks to the usage of active suspension systems. A similar strategy has used to improve the bending behaviour of the trains and reduce the acceleration sensed by passengers in train bogies. As result of these criteria , the cost of system , the complexity of design and the energy requirements increase [3][4].
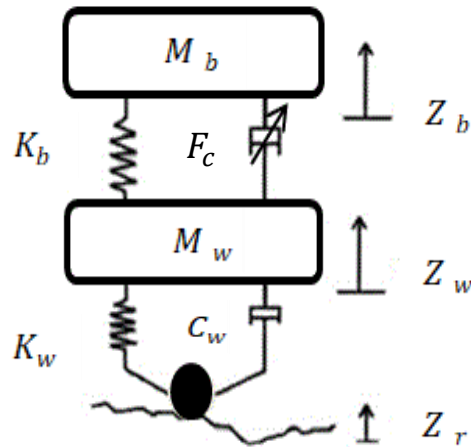
Figure 1-3: Active suspension system

1.2.3 Semi-Active Suspension System

The first semi-active suspension was proposed by Karnopp et al. in 1973 [5]. A semi-active suspension model is shown in figure (1-4). By using an controller unite, Fmr may generate an active actuating force. Since then, semi-active suspension systems have grown in favor in applications for vehicle suspension systems due to their greater efficiency and benefits above passive suspension systems. The damping properties of the damper can be modified to some extent in semi-active suspension systems. Semi-active dampers use a range of technologies to provide customizable damping properties, including solenoid valves, piezoelectric actuators, and electro- and magnetorheological (ER, MR) fluids[6].
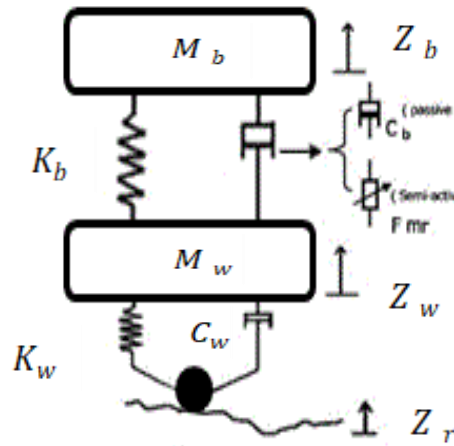
Figure 1-4: Semi-active suspension system.

There are two parts to a semi-active suspension: passive and semi-active. To manage the suspension system, the semi-active portion receives damping force from an external power supply called an actuator (e.g., electrical linear motor or hydraulic cylinder). A damper, a spring, or other comparable components, are used in the passive section. The advantage of this section is required in some systems, although it can also be removed. There are two types of suspension systems: high-bandwidth and low-bandwidth systems.

The parallel connection between the active and passive components of the suspension system is known as the Low-Bandwidth Configuration (LBC). The active suspension system may control the height of the automobile body (sprung mass) using the LBC design. However, because it supports the static load, the first limition of this technique is that the actuator cannot be removed or switched off. The another drawback, it is only effective at low frequencies. High-Bandwidth Configuration (HBC), on the other hand, can be regulated at frequencies higher than those of low-bandwidth configuration (LBC), and the passive component can continue to function even if the active component fails. The only disadvantage of HBC is that it cannot successfully manage

vehicle height. Active and passive components are linked in parallel in an HBC setup. HBC's motion equations are nearly identical to those of LBC, with the addition of an actuator force .

MR dampers are a type of semi-active control system. that provide controllable damping by using MR fluids. These kinds have the potential to provide extremely dependable performance and can be considered fail-safe since they serve as passive dampers in the event that the control hardware malfunctions. Models that can appropriately define the damper's intrinsic nonlinear behaviour must be established in order to create control algorithms that fully use the special features of the MR damper[6].

1.2.3.1   ER and MR Fluids

Many researchers have recently looked into the potential applications of electrorheological (ER) and magnetorheological (MR) fluids in controlled dampers. ER and MR fluids are intelligent materials that combine small particles with low-viscosity liquids. In the presence of a strong electric or magnetic field, the particles will create chain-like fibrous formations, As show in figure (1-5). The suspension will solidify and have high yield stress when the intensity of the magnetic or electric field reaches a specific level; however, the suspension can be liquefied again by removing the electric field or magnetic field. The change process is very fast, takes only a few milliseconds, and is quite easy to manipulate. The energy consumption is also minimal, consuming only a few watts. In the 1940s, ER and MR fluids were invented separately [8]. ER fluids attracted the greatest attention initially; however, they were subsequently discovered to be less well-suited to most applications than MR fluids.

(a)   (b)
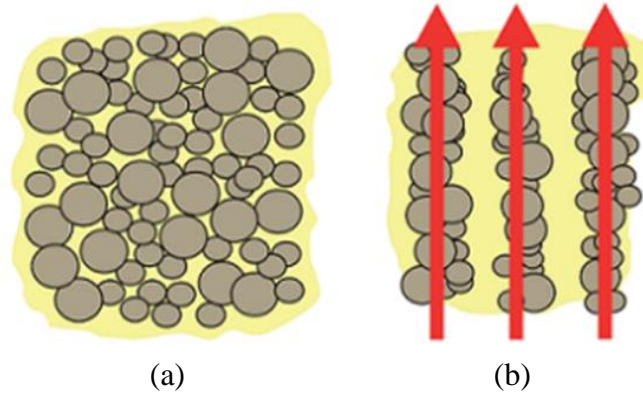
Figure 1-5: Magnetorheological (MR) fluids[7]

(a) without magnetic field (b) with magnetic field

All MR and ER fluids have identical viscosity in their nonactivated or "off" states; however, MR fluids have a far larger rise in yield strength and lower viscosity than their electric counterparts. The higher yield stress for ER fluid is around 10 kPa, while the MR fluid can reach around 100 kPa[9].

Table 1-1: Comparative between MR and ER fluid[12].

Property	MR Fluid	ER Fluid
Temperature Range	-40 to 150 C^0	+10 to 90 C^0
Stability	Unaffected by Most Impurities	Cannot Tolerate Impurities
Density	3 to 4 g/cm^3	1 to 2 g/cm^3
Max. yield Stress	50 to 100 kPa	2 to 5 kPa
Max. field	~250 kA/m	~4 kV/mm
Power Supply (typical)	2 to 25 V & 1 to 2 A	2000 to 5000 V & 1 to 10 A

1.2.3.2 MR Damper

An MR damper works similarly to passive hydraulic dampers in that it uses fluid to flow between chambers through small holes in the piston, transforming "shock" energy into heat. In an MR damper, however, an electrical connection is included in the piston assembly. A coil inside the piston generates a magnetic field when an electrical current is applied to the damper, quickly altering the MR Fluid's properties in the piston figure (1-6). As a result, by changing the electrical current to the damper, the resistance of the damper can be continually altered in real time[10].
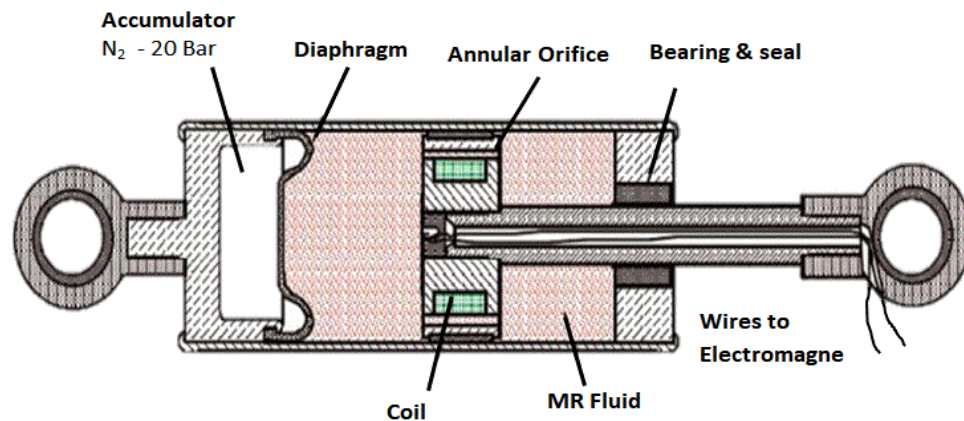
Figure 1-6 : MR damper diagram[11].

MRDs (magneto-rheological fluid dampers) are excellent structure vibration control devices depending on the magneto-rheological fluid's immediate and reversible rheological effect (MRF). MRDs are widely employed in various technical domains because of their damping force controllability. According to results of researchers, semi-active vehicle suspension systems depending on MRDs are more successful than passive suspensions in improving

8

manoeuvrability and ride performance; therefore, vehicle MRDs have gotten much attention in recent years. The essential performance indexes for MRDs' dynamic features are damping force and response time, which determine MRDs' application and working system. We expect MRDs to have a higher adjustable damping force and a shorter response time to achieve superior real-time control effects. According to related research, the damping force of MRDs varies substantially due to differences in size parameters and geometries, and the response time varies from tens to hundreds of milliseconds depending on the testing condition[11].

Table 1- 2: Comparative between active, semi-active, and passive system.

Passive system	Active system	Semi-active system
Passive dynamic behavior	Dynamic behaviour is effective	Dynamic behavior is lower to active behavior
Simple structural design	Complex structural design	Structural design is more complex than passive
Riding comfort and road maneuvers are very poor	Riding comfort and road maneuvers are good	The ride comfort and road maneuvers are better than the passive and are considered good and acceptable
excellent reliability	Low reliability compared to passive and semi-active	high reliability
low cost	Very high cost	medium cost compared to active and passive
Does not need external power	High power required	Less energy is required compared to active

1.3 Aim Of The Thesis

This thesis aims to investigate parametric techniques for identifying the nonlinear dynamics of an MR damper and Implement these techniques in the investigation of MR damper control of a vehicle suspension system that makes minimal use of sensors, thereby reducing the implementation cost and increasing system reliability. Four modern parametric models were selected, and a comparison was made in simulating the behaviour of the MR damper.

1.4 Steps for Achieving the Aim

The main objectives of this thesis are represented by the following.

1- Studying the classifications of vehicle suspension systems and comparing them.

2- A comprehensive review of the semi-active suspension systems with studies on the installation and working method of MR dampers.

3- A focused study of the essential parametric models that explain the hysterical behaviour of the MR damper.

4- Modelling of the passive suspension system with the use of three types of road shapes.

5- Simulation of MR damper models using a constant voltage of 1.5 V.

6- Modelling of a controller capable of controlling the value of the voltage supplied to the MR damper with the choice of the Skyhook technique to represent the system control with HSF technology representing the damper control.

7- Analyzing the results obtained by simulating the semi-active suspension system and comparing them with the passive suspension.

1.5 Thesis Layout

- Chapter one provides an overview of suspension systems and their classifications and represents the introduction to this thesis.

- Chapter two reviews previous studies on suspension systems in vehicles, focusing on semi-active systems.

- Chapter three presents the theoretical description of the semi-active quarter-car suspension model with a review of the mathematical formulas of the parametric models and the control module used in the MR damper.

- Chapter four discusses the simulation results for semi-active and passive suspension systems using Matlab/Simulink.

- Chapter five reviews the conclusion with the recommendation

Chapter Two

Literature Review

Chapter 2. Literature Review

2.1 Introduction

In this chapter, Most of the literature related to improving vehicle suspension systems is reviewed and everything related to quarter-car models. Moreover, reviewing the analytical models of the MR dampers that have been proposed.

2.2 Classification Of Vehicle Suspension Systems

All researchers seek to design a suspension system that completely isolates the vehicle from road influences. Suspension systems classify vehicles into passive, active and semi-active see Figure (2-1). This chapter will emphasize the literature on semi-active suspension systems[13].
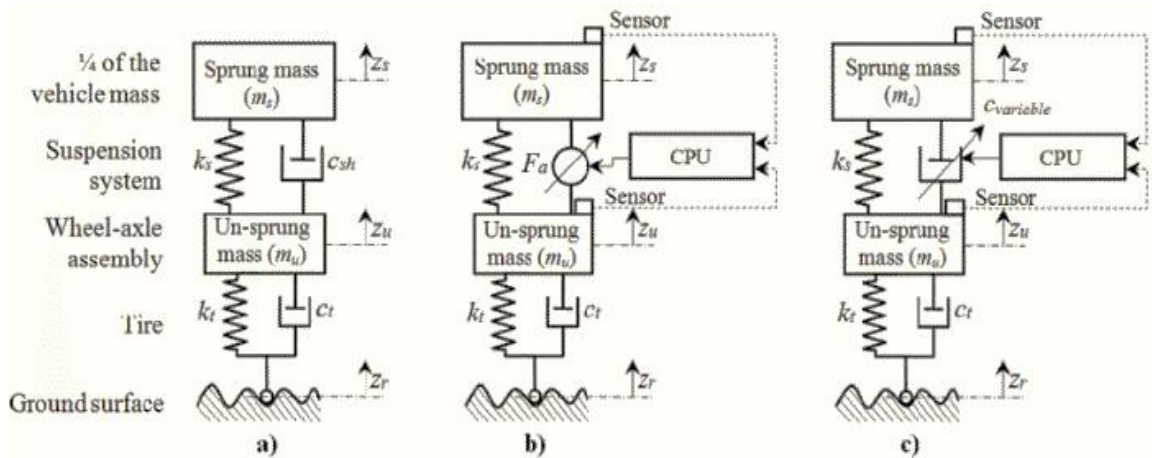
Figure 2–1: Sketch diagram of suspension system [13].

(a)Passive (b) Active (c) Semi-Active

2.2.1   Passive Suspension System

Passive suspension systems are considered one of the most widely used systems in the automotive industry due to their high reliability and low cost. They contain a spring with a Passive damper. These systems give stable and specific damping properties. See figure (2-1a).

A.C. Mitra et al. [14] studied a simulation model based on the Box–Behnken architecture of RSM to analyse ride comfort with correct independent variables. Regression analysis is used to create a prediction model for the response variable, RC, which has a high level of agreement with the simulated model (R2 = 99.74%). The response analysis used the quarter-car model with the help of the Matlab/Simulink program.

Ali I. H. Al-Zughaibi[15] proposed a new nonlinear friction model using a quarter-car passive suspension system. Through the experimental results and the dynamics system analysis. The proposed model includes most of the friction behaviours that appeared in the test results, as it is considered more accurate than the simple friction model. Figure (2-2) shows a device that is designed to simulate the practical results of the model.
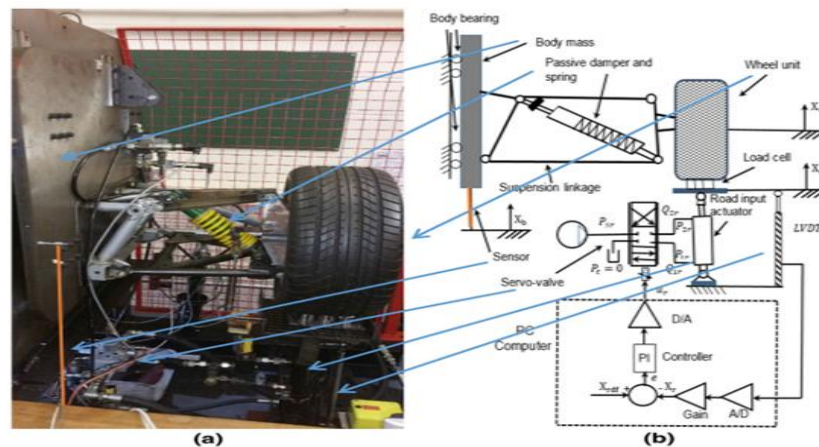
Figure 2-2: (a) Photograph of the test rig. (b) Road simulator and
testing equipment schematic[15].

15

2.2.2   Active Suspension System

Active suspension systems are considered one of the best systems that give satisfactory results in damping vibrations. The passive elements in the suspension systems are replaced by a control element that gives strength to the system and is called an actuator. The actuator represents one of the most critical parts of a system and can be classified as an electromagnetic actuator, pneumatic, and hydraulic actuator. Some Literature reviews were given about this system[17].

P. Dowds and A. O'Dwyer [16] studied the modelling of active and passive damping using a quarter-of-a-vehicle and a full-vehicle model. While compared to the passive suspension system, the active suspension system allows for a much-improved regulator response, As shown in figure (2-3). The actuator's power usage is the most significant practical difficulty in establishing active suspension. The actuator is typically the controlling component of an active suspension.
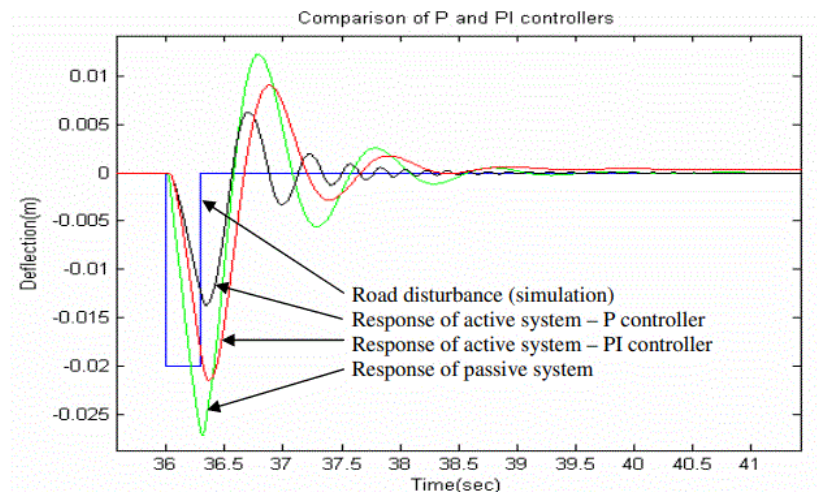
Figure2-3: Suspension response for both passive and active system[16].

Amit A. Divekar and Bhushan D. Mahajan [18] focused on the development of control algorithms for suspension systems for a quarter car (2DOF) by proposing a control system to reduce the sprung mass displacement and known as Fussy Logic (FLC) control with the use of MATLAB/Simulink. Program to simulate the response results. It compared the proposed control system with the traditional PID, showing that the Fussy PID control device has better results.

S.Kilicaslan et al. [19] studied using ASRE and SDRE techniques to nonlinear control ASS are present in this work and used a quarter-car suspension model of a Ford Fiesta Mk2. The simulations suggest that the regulation of ASS utilising SDRE and ASRE approaches give good results. Both approaches' simulation results are compared to the PSS equivalent. Both SDRE and ASRE approaches are effective in meeting performance requirements.

Sellami et al. [20] proposed the Luenberger observer approach in this study to design automobile active suspension systems. The key idea is to employ a bond graph approach to diagnose utilising the observer. Where it is displayed an article on the bond graph tool's efficacy in modelling industrial systems based on its structural qualities and ease of use as a graphical tool; provided us with a better representation of the physical system.

2.2.3   Semi-Active Suspension System

The semi-active suspension system contains a spring and damper with variable damping characteristics. The most important characteristic of this system is that it turns into a passive system when a malfunction occurs in the control system; this shows high reliability. Some literature reviews of semi-active suspension systems and MR dampers will be present in this part. In

order to analyze the dynamic nonlinear behaviour of MR dampers, there are both parametric and non-parametric methods.

LV Hongzhan et al.[21] investigated the Bouc-Wen model, the modified Bouc-Wen model, the viscoelastic plastic model, and the hysteresis bi-viscous model. The experiment served as the foundation for the four models. Tests are used to measure the magnetorheological damper's mechanical characteristics. This study showed that, among parametric models, the revised Buoc-wen model had the highest accuracy in explaining the behaviour of MRD, As shown in figure (2-4). At lower speeds, the prediction error for the damping force is more significant.
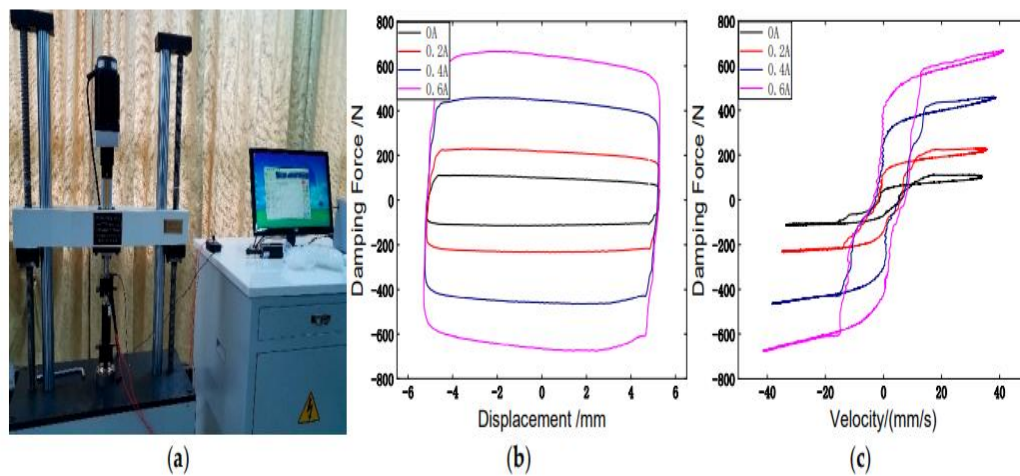
Figure 2-4:The hysterical behavior of the Bouc-wen model with voltage variation[21].

(a) test device (b) force-displacement diagram (c) force-velocity diagram

Tieshan Zhang and Zhong Ren [22] examined the dynamical models of the magnetorheological damper. The expanded Bingham model was frequently employed. After that, the simulation was run, and the benefits and drawbacks of the two models were compared (Figure (2-5)). Last, a novel dynamical model based on the tangent function was presented. A simulation was used to show the parameters' physical significance. The simulation results

demonstrated that the new model's curve was accurate and smooth. The simulation and research of the magnetorheological damper may be done using it.
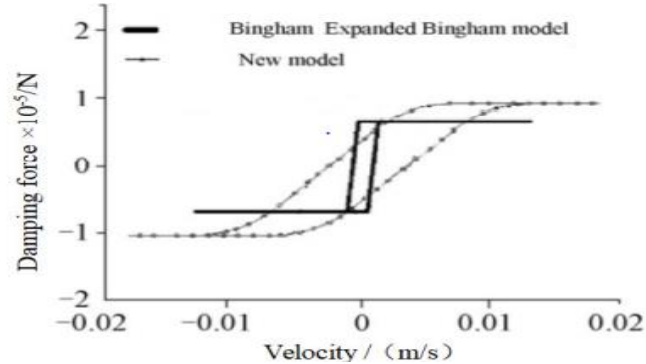
Figure 2-5: The force-velocity diagram for two models[22].

Tu, Fengchen, et al [23] presented an experimental study of semi-active suspension systems (MRD) with the structural design of the MR damper, which was tested with the experimental results of the damper. The magnetic circuits are well-designed with the structure for the MR damper. Figure (2-6) shows the test results and their comparison with the relevant result.
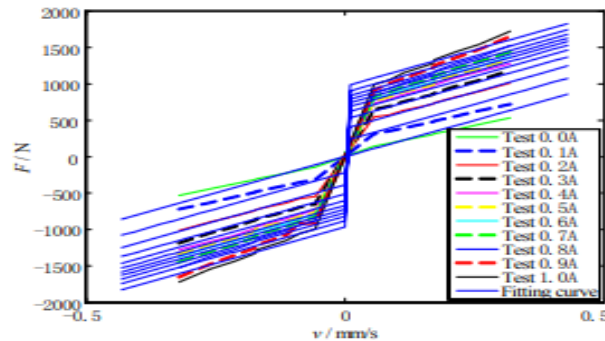
Figure 2-6: force-velocity diagram between experimental and analytical results[23].

Amit A.Hingane et al. [24] Showed a brief comparison between the semi-active and passive suspension systems. A Bingham model with an MR damper was selected to be tested with the quarter car model (2DOF), and the results were simulated by MATLAB/Simulink program. The results showed a clear

improvement in decreasing the acceleration of the spring-mass when using the MR damper.

Şahin et al. [25] manufactured and tested the MR damper as shown in figure (2-7), where eight parametric models were used to explain the behaviour of nonlinear MR dampers. Also, an evaluation was made between three parametric algebraic models and five ordinary differential parametric models. The results showed that the parametric algebraic models better predict the hysterical behaviour of the damper MR.

Choi, Seung-bok et al. [26] have compared the measured and predicted damping strength of the Bingham, Buoc-wen and the polynomial proposed model. The two results show that the Bingham model provides good damping power, but it cannot predict all behaviours of the MR damper. On the other hand, either the Buoc-wen or polynomial model has predicted the nonlinear behaviour of the MR damper well.

2.3 Semi-Active Vibration Control Strategies

Because the MR damper can only be directly instructed to change the voltage applied to its electromagnet, as a result, in a control system that determines the damper force necessary for the system to respect a reference model, a damper controller is also necessary. For the damper's actual force fa to match the desired force fd, this controller calculates the voltage v that should be supplied. Some control strategies developed and tested for the system controller include H control, fuzzy logic control, flexible neural network control, Skyhook control, linear quadratic Gaussian control, and sliding-mode control robust control[27].

Haiping Du et al. [28] studied how an MR damper is adapted to a quarter-car model in conjunction with a polynomial model derived from testing data and an appropriately built static output feedback H∞ controller shown in figure (2-8). The performance of this technique, as tested by numerical simulation, has proven that despite its simplicity, With the polynomial model of the MRD and the static output feedback H∞ controller, equivalent performance to active suspension can be achieved.
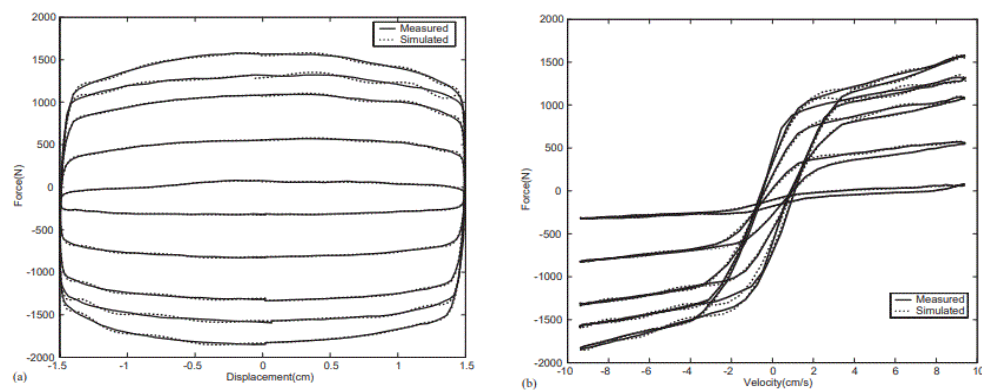
Figure 2-8: Comparison of practical and analytical results of MRD behavior[28].

Ahmed E. et al. [29] developed semi-active suspension systems using PSO and LQR technology as a system control unit using the Matlab/Simulink environment. By comparing the simulation results, it was concluded the PSO technique gives better and more accurate results to improve the performance of the car suspension while reducing vibrations.

K.Dhananjay Rao [30] suggested used a MATLAB Simulink model to evaluate the effectiveness of a semi-active system for a quarter automobile model utilising a PID controller. This study's dynamic system is linear. Essential vehicle suspension performances like wheel displacement, wheel deflection, suspension travels, body acceleration, and body displacement can be captured using a linear system. The system takes two types of road profiles.

According to the results, the proposed PID controller enhances the body and wheel displacement performance.

Alisina S.et al.[31] studied theoretical and experimental for semi-active suspension systems in a quarter-car model with control units was presented. It was used in the Skyhook, fuzzy and On-Off control systems, and the damper control unit was represented by Havsid technology. Figure (2-9) shows the simulation results for the control techniques with the MR passive suspension system.
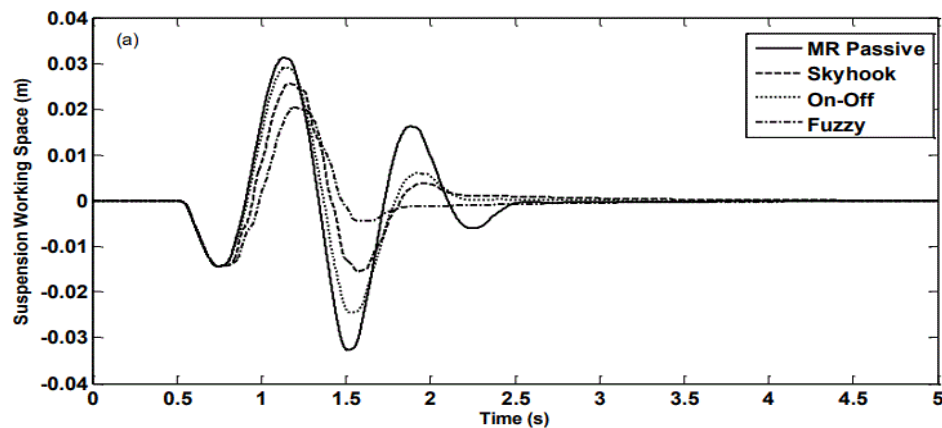
Figure 2-9: The response of the suspension system with the different type of control system[31].

2.4   Summary

This chapter reviews some literature specialising in automobile suspension systems, concentrating on semi-active suspension systems that use MR dampers. The main objective of the previous literature is to reach a dynamic model that explains the behaviour of the MR damper with high accuracy in order to be used practically. On the other hand, this field is

complicated because of the non-linear behaviour of MR fluids, which are non-Newtonian fluids. From the literature reviewed, it was concluded that the parametric models are the most polarising for researchers because of the theoretical physical behaviour through which the hysterical interpretation of the MR damper is interpreted.

In this thesis, a comparison will be made between the most widely used parametric models used by researchers to explain the hysteretic behaviour of the MR damper. The comparison is made by using a different input signal on the quarter car model to test the response of the MR damper between the parametric models with a suitable control unit for the simulation process. On the other hand, this study represents a comprehensive review of the semi-active suspension system using the MRD technique

Chapter Three

Theoretical

Chapter 3. Theoretical

3.1 Introduction

The purpose of this chapter is to describe the theoretical aspects of simulation semi-active suspension systems using an MR damper. In order to understand the hysterical behaviour of MRDs, many mathematical models have been reached in the past years. This description includes four essential parametric differential models with the quarter-car model. A control unit must be used to reach a semi-active suspension that can be controlled. The bouc-wen model is simulated with a skyhook control system and damper control represented by SFM to improve the damping of the vibrations caused by the road profile.

3.2 Quarter-car model

To the best knowledge of the MRDs, the model must be simulated with the car's suspension to reach accurate results. The QCM was chosen for simulation because of the simplicity of the design with more accurate results, shwn in figure (3-1).
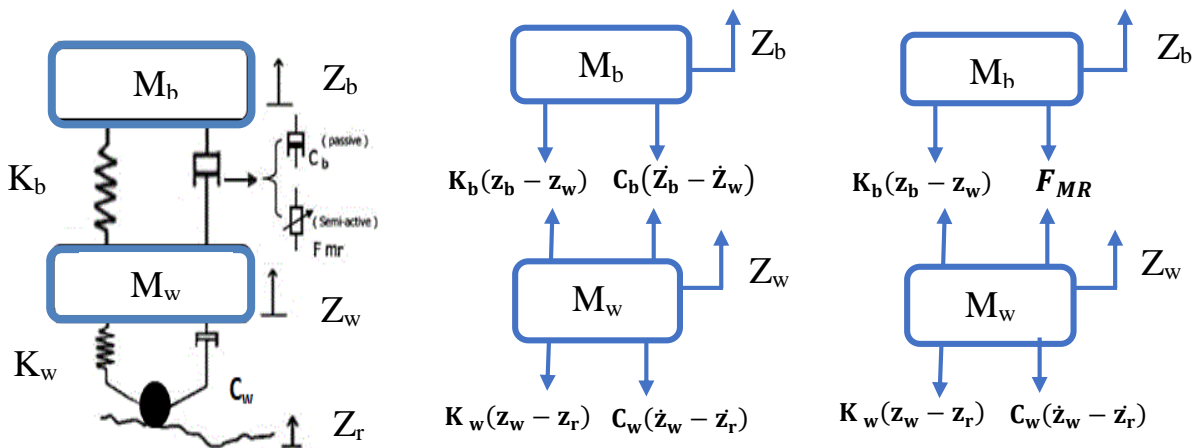
Figure 3-1: a) Quarter-car model b) free budy digram for passive c) free budy digram for semi-active.

The model includes both the mass of vehicle body M_b and the tires M_w, where Newton's second law can be used to express the movement of both masses with mathematical equations as follows.

a) passive suspension model

$$M_b \ddot{z}_b = -K_b(z_b - z_w) - C_b(\dot{Z}_b - \dot{Z}_w) \tag{3.1a}$$

$$M_w \ddot{z}_w = K_b(z_b - z_w) - C_w(\dot{z}_w - \dot{z}_r) - K_w(z_w - z_r) + C_b(\dot{Z}_b - \dot{Z}_w) \tag{3.1b}$$

b) semi-active suspension model

$$M_b \ddot{z}_b = -K_b(z_b - z_w) - F_{MR} \tag{3.2a}$$

$$M_w \ddot{z}_w = K_b(z_b - z_w) - C_w(\dot{z}_w - \dot{z}_r) - K_w(z_w - z_r) + F_{MR} \tag{3.2b}$$

When $\quad F_{MR} = F + C_b(\dot{Z}_b - \dot{Z}_w) \tag{3.2c}$

A spring mass (M_b)and an un-spring mass (M_w), respectively, tyre stiffness (K_w), spring stiffness, and passive damping coefficients (K_b and C_b), are all included in the model. The displacements x_b and x_w of the quarter-vehicle model specify its vertical motions, whereas Z_r represents the excitation brought on by undesirable road irregularities. The data utilized in this investigation are presented in Table 1, which was supplied in [33].

Table 3-1 : Quarter-Car coefficient values[33]

No.	coefficient name	coefficient notation	coefficient value
1	Sprung Mass	M_w	380(kg)
2	Un-sprung Mass	M_w	31(kg)
3	Stiffness of Suspension	K_b	29,000(N/m)
4	Stiffness of Un-spring Mass (tire)	K_w	228,000(N/m)
5	Coefficient of Damping of Sprung Mass	C_b	1500(N-s/m)
6	Coefficient of Damping of Un-sprung Mass	C_w	110(N-s/m)

3.3 Models For MR Fluids

As it was presented in Chapter one the MR fluids, has attracted many researchers. It is considered one of the innovative materials easily controlled

by a magnetic field, establishing its effectiveness in many applications. The main characteristic of MR fluids is the sizeable magnetic energy density that the fluid can create, which gives a significant, controllable dynamic stress. The behaviour of MRF is classified into the pre- yield and post- yield region, two distinct areas on which the behaviour of the MRFs depends. The pre-yield area is represented by viscoelastic material, which shows strong hysteresis, while the post-yield area is represented by plastic material with non-zero force. The intelligent material family includes magnetorheological (MR) fluids because a magnetic field can considerably change their rheological characteristics shown in figure(3-2) [34]. In a non-magnetic carrier fluid, they are suspensions of microscopic magnetically permeable particles. Carbonyl iron particles or ferromagnetic binary alloys like CoNi, FeCo, etc., are the most widely utilised suspended magnetic particles, and mineral oil, silicone oil, polyesters, and polyethers are the most frequent carrier fluids [35][36].

Without Magnetorheological Fluid   With Magnetorheological Fluid
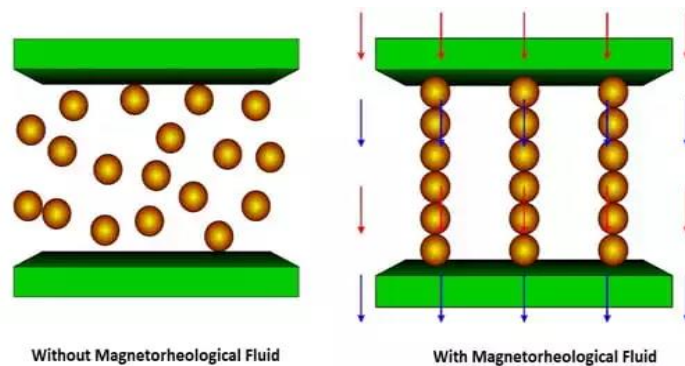
Figure 3-2: MR fluids[32].

The design of MR fluid devices involves the use of models for MRFs. Since Phillips [37] 's work investigated Bingham flows in channels with parallel walls and produced nondimensional versions of the Bingham flow equations, modelling MRFs has attracted significant attention. As a result, the level of accuracy offered by existing models is excellent. A broad range of nonlinear models, such as the Bingham plastic model [38], the Herschel–Bulkley model

[39], and the biviscous model [40], have been employed to describe MR fluids.

3.3.1   Bingham Plastic Model

A variable rigid, completely plastic element and a Newtonian viscosity element are included in the knows Bingham model of an MRF, establishing the essential relationship between stress and strain to be represented in equations (3.3) [41].

$$\tau = \tau_y(H)\text{sgn}(\dot{\gamma}) + \eta\dot{\gamma} \qquad\qquad (3.3)$$

Where τ is the fluid's shear stress, τ_y is the yielding shear stress regulated by the applied magnetic field H, sgn( ) is the signum function, η is the fluid Newtonian viscosity, and $\dot{\gamma}$ is the shear strain rate. In other words, When the shear stress is less than the crucial value τ_y, the fluid is at rest and behaves viscoelastically, at which point it behaves like a Newtonian fluid and flows. Figure (3-3) illustrates the Bingham plastic model to explain the behavior of the yield stress that is depending on the field.
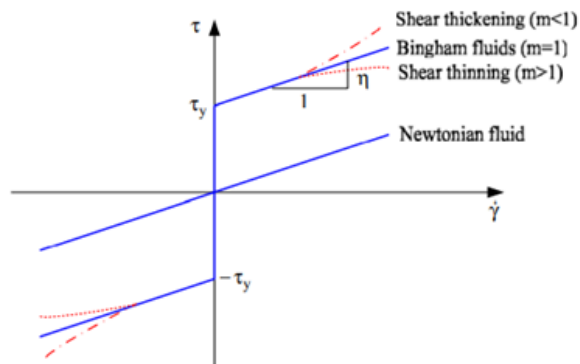
Figure 3-3: Bingham plastic model to describe MR fluids[41].

3.3.2 Biviscous Model.

In this model, the Bingham plastic equation that controls the shear stress τ has been generalized to describe MR fluids operating in squeeze flow mode shown in figure (3-3).

$$\tau = \begin{cases} \tau_y(H) + \eta\dot{\gamma} & |\tau| > \tau_1 \\ \eta_r\dot{\gamma} & |\tau| > \tau_1 \end{cases} \qquad (3.4)$$

Thus, as seen in figure(3-4), η_r and η refer to, respectively, the elastic and viscous fluid characteristics. $\tau_y(H)$ and τ_1 satisfy the yield parameters.

$$\tau_y(H) = \tau_1\left(1 - \frac{\eta}{\eta_r}\right) \qquad (3.5)$$

The Bingham model should be viewed as a limiting version of the biviscous model, Wilson pointed out [42]. For $\eta_r \to \infty$, the Bingham plastic model is obtained.
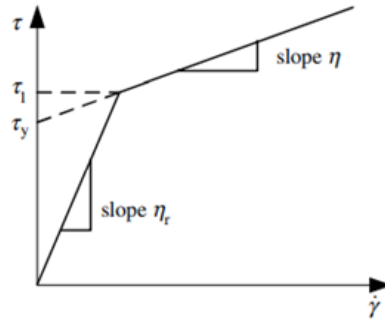
Figure 3-4: Idealized biviscous constitutive relationship[40].

3.3.3 Herschel–Bulkley Model

The Herschel-Bulkley model is an alternative to the Bingham model and is estimated to account for MRFs' post-yield shear thinning or thickening

behaviour. As shown in figure(3-3), the Herschel-Bulkley model may be described [38][39].

$$\tau = \left(\tau_Y(H) + K|\dot{\gamma}|^{\frac{1}{m}}\right)\text{sgn}(\dot{\gamma}) \qquad\qquad (3.6)$$

where the fluid parameters K and m. equations (3.4) describes a shear-thinning fluid for $m > 1$, whereas $m < 1$ describes shear-thickening fluids. Keep in mind that the Herschel-Bulkley model becomes the Bingham plastic model when $m = 1$.

3.4 MR Dampers Models

In addition to what was mentioned in the first chapter of this study about MR dampers, A hydraulic cylinder, magnetic coils, and MRFs make up an MR damper, which offers a straightforward construction. As well as to design simplicity and field controllability, Other benefits of MRDs Are:

A. Relatively low power input requirements [40][41].

B. Rise yield stress up to 100 kPa.

C. Stable operation in a wide temperature range (40-150 C).

D. Non-toxic and impervious to contaminants MR fluids.

The MRD may operate in a fail-safe mode, as a conventional passive dashpot, without the magnetic field. Due to these benefits, MR dampers have attracted much attention from a variety of application domains, including but not limited to knee prostheses, seismic vibration reduction [43], Hydraulic valves [44], massive bridge vibration management, and automobile suspensions [45,46,47,48]. The effectiveness of MR dampers in reducing free and forced cable vibrations is numerically explored and assessed as one application of the model [49]. However, effective control requires understanding the

nonlinear hysteretic behaviour of an MR damper under a magnetic field. As a result, it is necessary to create control algorithms that fully exploit the special qualities of MRDs, and the models must accurately capture the intrinsically nonlinear behaviour of these components.

The models now in use may be divided into two primary groups: parametric and nonparametric. Nonparametric models can simulate the behaviour of MR dampers without requiring that the model's parameters have any particular physical significance [50]. Polynomial model [51][52], and neuro-fuzzy [53],query-based model [54], neural networks [55][56], black-box model [57][58], Ridgenet model [59] are a few examples of nonparametric models. Sizable experimental datasets for model validation, even if they can become effective. According to a literature review, nonparametric models are quite complex and need to capture the behaviour of MR dampers.

On the other hand, parametric models are preferred since their parameters have some physical significance. The mechanical components of these models include linear viscosity, friction, springs, and others. By contrasting the models with the outcomes of the experiments, parameters related to these mechanical factors are calculated [60].

In previous years, parametric models were created and developed to predict magnetic resonance dampers' behaviour. The main objective is to interpret and simulate the hysterical behaviour of the damping force. Where parametric models are categorized as follows: the Bingham model[60], the LuGre hysteresis dynamic model [60][61], the viscoelastic–plastic models [62], the equivalent models [63], the Bouc–Wen hysteresis dynamic models [64][65][66], the biviscous models [66], the Dahl hysteresis dynamic

31

models[67], the hyperbolic tangent models [68], the stiffness–viscosity elasto-slide models [69], the sigmoid function-based models [70], and the phase transition models [71].

3.4.1 Bingham Model-Based Dynamic Models

3.4.1.1 Simple Bingham Model(SBM)

The Bingham plastic model was created by Stanway et al. [72] and included a Coulomb friction component running parallel to a viscous dashpot to describe the electrorheological (ER) damping mechanism, as illustrated in figure (3-5a). The damping force for MRDs can also be modelled using the nonlinear Bingham plastic model [60]. Figure (3-5a) shows that the force produced by the MRDs is provided by

$$F_{MR} = F_c sgn(\dot{x}) + C_0\dot{x} + F_0 \qquad\qquad (3.7)$$

where F_0 is the offset in the force applied to represent the force's observed non-zero mean caused by the accumulator's presence, C_0 is the damping parameter, F_c is the frictional force referring the yield stress that depends on the field, and x denotes the velocity pertaining to the external excitation. The Bingham behaviour of an MR damper is inferred from the Bingham plastic model for MR fluids defined by equations (3.3) [73] by examination of an axisymmetric model of the MR fluid flow.

The Bingham model considers MR fluids' behaviour after the yield point, i.e., fully realized fluid flow or considerable shear rates. However, it assumes that the fluid is stiff in the area before it yields. Therefore, the Bingham model does not describe the fluid elastic characteristics at small deflections and low shear rates, which are required for dynamic applications [74].

Since the release of the simple Bingham model describing the behaviour of MR dampers, many researchers in the field have attempted to develop this model to increase the predicted hysterical cycle. Therefore, displaying some of these works is okay: the following.
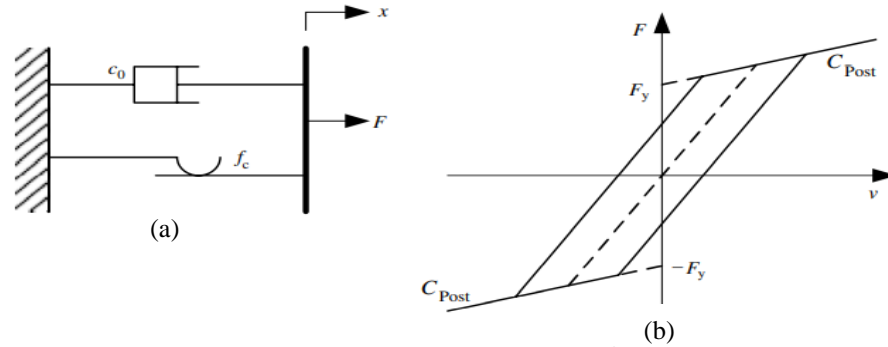
Figure 3-5: Simple Bingham model for MRD (a) parallel Coulomb friction component with a viscous dashpot (b) Force-velocity behavior of the Bingham model [60].

3.4.1.2   Extension I of the Bingham Model

The polynomial Bingham model developed by Wereley et al. [75] is depicted in figure (3-5b), and the equations characterizing the damper model are.

$$F(t) = \begin{cases} C_{post}\dot{x} + F_y & \dot{x} > 0 \\ -F_y < F(t) > F_y & \dot{x} = 0 \\ C_{post}\dot{x} - F_y & \dot{x} < 0 \end{cases} \qquad (3.8)$$

Where F_y is the yield force, and C_{post} is the post-yield damping. Equation (3.8) Bingham plastic model for MRDs is frequently written as

$$F_{MR} = C_{post}\dot{x} + F_y sgn(\dot{x}) \qquad (3.9)$$

The model provided by equation (3.9) makes the assumption that the material is stiff and does not flow in the pre-yield stage; as a result, when $|F(t)| < F_y$, the shaft velocity $x = 0$. The substance is fundamentally a non-zero Newtonian fluid, yield stress occurs when the damper is subjected to a force

33

greater than the yield force, as shown in figure(3-5b). Figure(3-5b) illustrates how the yield force in this constitutive model is calculated from the post-yield force vs. velocity intersection with the force axis[60].

3.4.1.3 Extension II of the Bingham model

In order to predict the behaviour of ER materials, Gamota and Filisko [76] created the Bingham model, which Spencer et al. used to simulate the dynamics of MR dampers. As shown, the governing equation is

$$F_{MR} = k_1(x_2 - x_1) + c_1(\dot{x}_2 - \dot{x}_1) + F_0 = c_0\dot{x}_1 + f_c sgn(\dot{x}_1) + F_0$$

$$= k_2(x - x_2) + F_0 \qquad\qquad |F_{MR}| > f_c \qquad (3.10)$$

$$F_{MR} = k_1(x_2 - x_1) + c_1(\dot{x}_2) + f_0$$

$$= k_2(x - x_2) + F_0 \qquad\qquad |F_{MR}| \geq f_c \qquad (3.11)$$

The following becomes clear to us through some of the papers in which the Bingham models were studied. Which showed that the Bingham model shown in equations (3.10) and (3.11) might represent the force-velocity behaviour of the MRDs. The proposed method of ordinary differential equations is quite stiff because of the nonlinear Coulomb friction element. As a result, relatively small time steps are needed for the numerical calculations using explicit integration methods. The equation (3.9) accurately represents the damping force in a nonlinear Bingham plastic model only in the post-yield region. On the other hand, the behavior of MR dampers in the pry-yield region is not explained. It seems that the Bingham model, one of the simplest and oldest models and a good description of the behaviour of force-displacement and force-velocity, has been effectively formulated shown in equations (3.7). However, based on the non-zero-piston assumption, this model does not adequately represent the damper's behaviour at speeds near zero.

3.4.2   Bouc–Wen Dynamic Models

Bouc [77] first proposed the Bouc-Wen hysteresis operator as an analytical definition of a soft hysteretical model, and Wen [78] afterwards generalised it. A vast class of hysteretic behaviour, ranging from inelastic stress-strain correlations present in structures to MRD behaviour [79], can be represented by the hysteresis model of Bouc, as refined by Wen, thanks to its appealing mathematical simplicity. The Bouc-Wen model has been widely used to simulate hysteresis loops because of including similar to force displacement velocity behavior of MR dampers analysis. In a nonlinear hysteretic system, the restoring force can be divided into two components:

$$F(x, \dot{x}) = g(x, \dot{x}) + \alpha z(x) \tag{3.12}$$

Where α is a scaling factor for the model, $z(x)$ is a hysteresis element that describes a function of the displacement's time, and $g(x, \dot{x})$ is a non-hysteretic part that provides a perform of the present velocity and displacement. z , a variable in evolution, is controlled by

$$\dot{Z} = -\gamma|\dot{x}|z|z|^{n-1} - \beta\dot{x}|z|^{n} + A\dot{x} \tag{3.13}$$

where the parameters $\gamma, \beta \ and \ A$ form the hysteresis loop and $\dot{Z}$ represents the time derivative and determine the size and overall Hysteresis loop's form, whereas n regulates the force-displacement curve's smoothness.

3.4.2.1   Simple Bouc–Wen Model(SBWM)

The Bouc-Wen hysteretic technician was used by Spencer et al. [80] to model the hysteretic behaviour of MRDs. figure (3-6a) illustrates the schematic of the suggested SBWM for MR dampers. The system's damping force is determined by

$$F_{MR} = C_0\dot{x} + K_0(x - x_0) + \alpha z \qquad\qquad (3.14)$$

Where the viscosity and stiffness coefficients, C_0 and K_0, are given, a spring's initial displacement x_0 was added to the model to account for the existence of an accumulator in the damper under consideration, and z is a different evolutionary controlled by equations (3.13). The force-velocity characteristic shape can be changed by modifying the parameter values, α, β, γ and n.

Because the resulting dynamic equations for the simple Bouc-Wen model are less stiff than the extended Bingham model, it is ideally suited for numerical simulation. However, it is unable to replicate the roll-off effect that has been experimentally observed in the yield region, that is, for low absolute quantity velocities with a functional sign that is the antithesis of the signal of the acceleration [60].

A group of eight constant parameters that connect the distinctive structure parameters to present excitation should be found in order to clearly define the behaviour of MR dampers using the SBWM provided by equations (3.13) and (3.14). This set of parameters is as follows:

$$\emptyset = [c_0, k_0, \alpha, x_0, \gamma, \beta, A, n]$$

3.4.2.2 Modified Bouc–Wen Model (MBWM)

It has been demonstrated that the mechanical idealisation of an MR damper presented in figure (3-6b) may correctly predict how it will behave given various inputs. The following equations control the phenomenological model presented by Spencer et al. [80]:

$$F_{MR} = \alpha z + c_0(\dot{x} + \dot{y}) + k_0(x - y) + k_1(x - x_0) \qquad\qquad (3.15)$$

Where z is the different evolutionary under the control of by

$$\dot{z} = -\gamma |\dot{x} - \dot{y}||z|^{n-1}z - \beta(\dot{x} - \dot{y})|z|^n + A(\dot{x} - \dot{y}) \qquad (3.16)$$

Where y is the internal displacement of the MR damper ruled by:

$$\dot{y} = \frac{1}{c_0+c_1}[\alpha z + c_0\dot{x} + k_0(x-y)] \qquad (3.17)$$

Where k_0 is provided to control the at high velocities, k_1 is the accumulator stiffness, c_0 and c_1 are the viscous damping seen at large and low velocities, respectively, and x_0 is employed to account for the effect of the accumulator. By γ, β, A, and n, the hysteresis loop's size and form can be changed.

A set of ten constant parameters that connect the distinctive structure parameters to current stimulation should be found in order to accurately describe a behaviour of MRDs using the MBWM provided by equations (3.15)–(3.17). and the following are the parameters:

$$\emptyset = [c_0, c_1, k_0, k_1, \alpha, x_0, \gamma, \beta, A, n]$$

All of the information we have previously investigated depends on how the MR damper responded. At the same time, the applied voltage and, consequently, the magnetic field were kept at a constant value. However, it is anticipated that the magnetic field would be continuously modified depending on the measured response of the system to which it is linked to obtaining the best performance of a control system using this device. To use the damper in this manner, a model that can forecast how the MR damper will behave in the

presence   of   a   changing   magnetic   field   must   be   created.

(a)   (b)
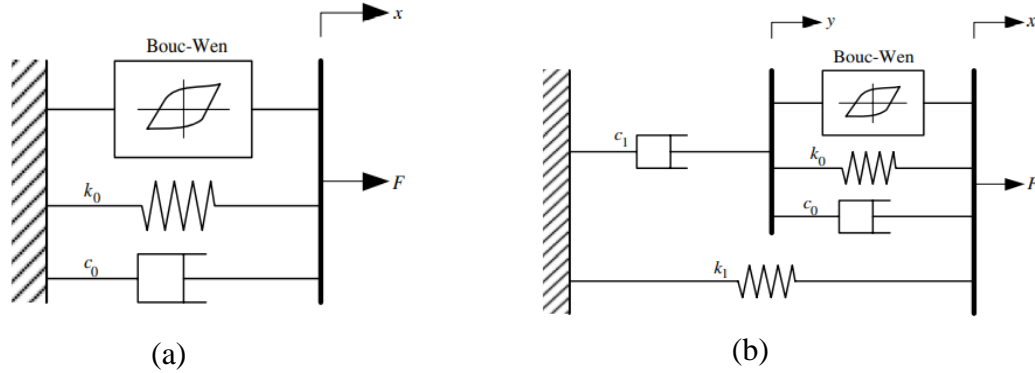
Figure 3-6: (a) Simple Bouc–Wen model (b) Modified Bouc–Wen model [81].

In order to obtain a parametric model that depends on the field change directly, Spencer et al. [80] formulated a mathematical relationship that relates the variables that depend on the current with the applied voltage(v), which are all of the following:

$$\alpha = \alpha(u) = \alpha_a + \alpha_b u \tag{3.18a}$$

$$c_1 = c_1(u) = c_{1a} + c_{1b} u \tag{3.18b}$$

$$c_0 = c_0(u) = c_{0a} + c_{0b} u \tag{3.18c}$$

where u is an internal parameter to assess the function dependency of the parameters on the applied voltage v ,and c_{0a} and α_a are the damping factor and Coulomb force of the MRD at 0 V. The first-order filter presented by models the link between u and v.

$$\dot{u} = -\eta(u - v) \tag{3.19}$$

where v represents the control voltage applied to the current driver, and η represents the MR damper's response time; a bigger η indicates a faster response time.

A set of 14 constant variable that link the distinctive shape variable to current excitation must be found in order to accurately define the behaviour of MRDs using the current-dependent Modified Bouc-Wen model presented by equations (3.15)-(3.19).

$$\emptyset = [c_{0a}, c_{0b}, c_{1a}, c_{1b}, k_0, k_1, \alpha_a, \alpha_b, x_0, \gamma, \beta, A, n, \eta]$$

The Modified Bouc-Wen model has been demonstrated to increase modelling accuracy [80]. However, a growing number of model parameters always increases model complexity, which may make it challenging to identify the parameters. As a result, only applications where an exact model is necessary employ this model. The modified Bouc-Wen model's main drawbacks are the possibility of errors brought on by the assumed linear current property and the challenges involved in identifying a high number of parameters[81].

3.4.3 Dahl Hysteresis Dynamic Models

For the aim of modelling control systems with friction, the Dahl model [82] was created. The author included a differential equation to model the stress-strain curve. Consider the displacement to be x, the friction force to be $f(t)$, and the Coulomb friction force to be f_c. The Dahl model is known as .

$$\frac{df(t)}{dx} = \sigma \left[1 - \frac{f(t)}{f_c} sgn(\dot{x})\right]^{\delta} \qquad\qquad (3.20)$$

Where σ is the stiffness parameter, δ is a constant, and δ is a parameter that affects how the stress-strain curve looks. The most typical value of $\delta = 1$, and larger values of δ result in a stress-strain curve with a bend more firmly. If the starting value of the friction force is such that$|f(0) < f_c|$, the friction force $|f(t)|$ will not be greater thanf_c .

For the case $\delta = 1$ and presenting $f(t) = \sigma Z$, the model can be rewritten as

$$\dot{Z} = \dot{X} - \frac{\sigma}{f_c}|\dot{x}|Z \qquad\qquad\qquad (3.21)$$

$$F(t) = \sigma Z \qquad\qquad\qquad (3.22)$$

where Z, a nonlinear filter-controlled internal hysteretic variable, is used.

Taking

$$\rho = \frac{\sigma}{f_c} \quad \text{and} \quad z(t) = \frac{\sigma}{f_c}Z(t) \qquad\qquad (3.23)$$

The Dahl model might be revised to write as

$$\dot{z} = \rho(\dot{x} - |\dot{x}|z) \qquad\qquad\qquad (3.24)$$

$$F(t) = f_c z \qquad\qquad\qquad (3.25)$$

The more generic hysteretic format presented by Bouc and Wen is a specific example of the hysteretic model provided by equation (3.21), which is attributed to Dahl [60].
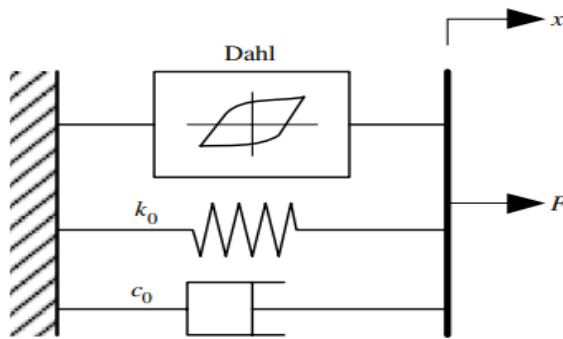
Figure 3-7: Modified Dahl model dynamic models[60].

3.4.3.1 Modified Dahl Model (MDM1)

Figure (3-7) shows the Dahl [82] model as modified by Zhou and Qu [83], which is simpler and more efficient. The Dahl hysteresis model rather than the Bouc-Wen model was used in this model to simulate the Coulomb force. Additionally, it was claimed that the modified Dahl model effectively captured the force-velocity connection in the minimal velocity range. The force produced by the MR damper in this model is given by:

$$F_{MR} = k_0 x(t) + c_0 \dot{x} + F_c z - f_0 \tag{3.26}$$

where x represents the displacement of the MR damper, c_0 the damping coefficient, k_0 the stiffness of the linear spring, F_c the Coulomb force modulated by the applied magnetic field, and f_0 the damper force brought on by seals and measurement bias. Where z is an equation-governed non-dimensional hysteretic variable governed by :

$$\dot{z} = \sigma \dot{x}(1 - z\, sgn(\dot{x})) \tag{3.27}$$

Where the hysteretic loop's form is determined by σ. It is required to determine the link between both the magnetic field applied and model parameters in order to configure the MDM1 under a specific supplied fluctuating magnetic field. This connection is established through equations (3.18). z Is a non-dimensional hysteretic parameters that is controlled by equation (3.27), and equations (3.18a) and (3.18c) can determine that the constants C_0 and α may be voltage-dependent.

To avoid determining too many variables, the MDM1 simulates the Coulomb force using the Dahl hysteresis function instead of the Bouc-Wen hysteresis function. This allows the modified Dahl model to accurately depict the force-

velocity connection in the low-velocity range. Therefore, eight variables should be specified for the suggested MDM1 for MR dampers. The set of variables is as follows:

$$\emptyset = [C_{0a}, C_{0b}, \alpha_a, \alpha_b, k_0, \sigma, f_0, \eta]$$

3.4.4   LuGre hysteresis Dynamic Models

To represent the friction dynamics, the LuGre hysteresis operator was given out in [84] and given that name in [85]. The LuGre hysteresis operator's friction has the following form.

$$F_{MR} = \sigma_0 z + \sigma_1 \dot{z} + \sigma_2 \dot{x} \tag{3.28}$$

Where, $\dot{x}$ is the relative speed between the two surfaces, σ_0 is stiffness, σ_1 is a damping coefficient, and z is an internal variable that reflects the average bristle deformation. The bristles' bending causes friction, which is described by the first two terms, and viscous friction, which is described by the third term, which is related to relative speed. Figure(3-8) Illustrates of the internal variable z presented by

$$\dot{z} = \dot{x} - \frac{|\dot{x}|}{g(\dot{x})} z \tag{3.29}$$

Where the positive function $g(\dot{x})$ is dependent on a variety of variables, including temperature, lubrication, and material characteristics.

$g(\dot{x}), \sigma_0, \sigma_2$ are correlated to the voltage by

$$g(\dot{x}) = \frac{1}{a_0 \, \sigma_{0b} \, \eta_0(v)} \tag{3.30}$$

$$\sigma_0 = \sigma_0(v) = \sigma_{0a} + \sigma_{0b} v \tag{3.31a}$$

42

$$\sigma_2 = \sigma_2(v) = \sigma_{2a} + \sigma_{2b}v \qquad\qquad (3.31b)$$

Where η_0 is a positive velocity function that explains the Stribeck effect, which is seen in friction phenomena at low velocities.
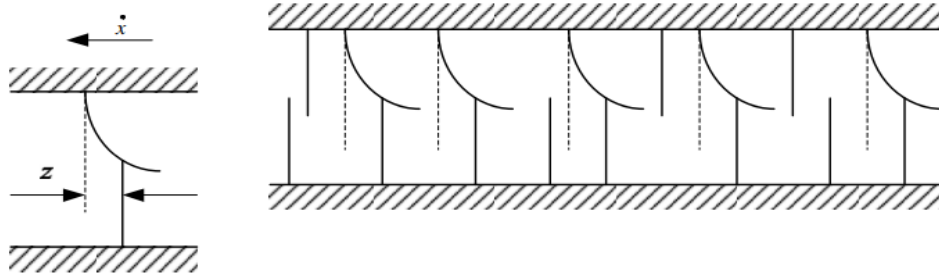
Figure 3-8: Bristle interpretation in the LuGre mode [60].

3.4.4.1   Modified LuGre Model I (MLGM1)

Alvarez [86] proposed a modified LuGre model to predict the dynamics of MRDs depending on the LuGre hysteresis function. Let

$$\sigma_{0a} = 0$$

The MR dampers' modified LuGre model has the following form:

$$F_{MR} = \sigma_{0b}\alpha a_0|\dot{x}|z(1 + a_1 v) \qquad\qquad (3.32)$$

$$\dot{z} = \dot{x}_1 - \sigma_{0b}\alpha a_0|\dot{x}|z(1 + a_1 v) \qquad\qquad (3.33)$$

where z is a parameter that can be interpreted as the average MRF transient deflection produced when the rod starts to move in one direction or the other (stiffness and damping coefficients, etc.). $\dot{x}$ is the relative speed between the damper's ends, $v(V)$ is the input voltage, and σ_0, σ_1, and σ_2 are constant variables refers to physical characteristics of the MRF.

A set of six constant variables that connect the distinctive shape variables to current excitation should be found in order to appropriately define the behaviour of MRDs using the LuGre model I for MRD provided by equations (3.31a) and (3.31b). This set of variables is as follows:

$$\emptyset = [\sigma_{0b}, \sigma_1, \sigma_{2a}, \alpha, a_0, a_1]$$

3.4.4.2   Modified LuGre Model II (MLGM2)

Sakai et al. [87][88] updated the LuGre model, provided by equations (3.32) and (3.33), for MRDs to describe the damping force. The inverse model was produced by providing a straightforward model for MRDs. In equation (3.34), the simplified LuGre model for MRD may be provided by assuming $\eta = 1$.

$$F_{MR} = \sigma_0 z + \sigma_1 \dot{z} + \sigma_2 \dot{x} \qquad\qquad (3.34)$$

$$\dot{z} = \dot{x} - \sigma_0 a_0 |\dot{x}| z \qquad\qquad (3.35)$$

A set of six variables that link the distinctive shape variables to current input should be found in order to correctly define the behaviour of MR dampers that use the LuGre model II for MRDs provided by equations (3.31a) and (3.31b).

$$\emptyset = [\sigma_{0a}, \sigma_{0b}, \sigma_1, \sigma_{2a}, a_0]$$

3.4.4.3   Modified LuGre Model III (MLGM3)

Jimenez et al. [89] described the dynamic behaviour of an MR damper using the modified LuGre friction model. This model, a development of Dahl's friction model, has been applied in various friction-related contexts. The mLF

model is a strong contender in modelling and controlling design issues due to its accuracy and mathematical simplicity. This is how the model is expressed:

$$F_{MR} = f_0 + \beta z + \gamma \dot{x} + \delta x + \varepsilon \dot{z} \qquad\qquad (3.36)$$

$$z = \dot{x} \overset{.}{-} \alpha |\dot{x}| z \qquad\qquad (3.37)$$

where the overall stiffness and damping parameters δ, γ, β and ε can change depending on the applied current. Also included are F(N), the overall force the MR damper applies, x (mm), the displacement of the damper, and z (mm), which describes the deflections of the MRF, which is really contained inside the damper cylinder.

However, for velocities close to zero, differences between experimental data and model reactions were seen [89]. This drawback is caused by the modified LuGre model's inability to adequately describe the Stribeck effect, which is crucial at low velocities.

3.5   MR Damper Behaviour

The basis of the semi-active suspension system is the ability to change the damping properties by controlling the value of the supplied current to create a magnetic field on the MR fluid. What characterizes the hysteretic behaviour of the MR damper is non-linear and changes with the current change. Therefore, the studied parametric models and the other models differ in terms of the hysterical loop picked up from the damper. In Figure (3-9), the force-velocity diagram of the behaviour MR damper is generally shown with the difference in the supplied current. Where the value of the current is 0A, the damping is the least possible and when the current reaches 2 A, the damping force becomes the highest possible, and this is the work of the semi-active

suspension. Through the force-velocity diagram, the hysterical behaviour of the MR damper models is evaluated. From one model to another, the amplitude of the stereo loop and the model's ability to predict the behaviour of the damper varies.
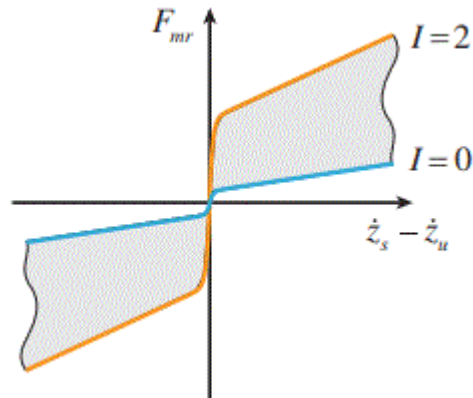
Figure 3-9: Overall force - velocity chart for semi-active suspension.

3.6 Vehicle Modelling And Control Objectives

The dynamics of a semi-active system are compelled to reach optimal circumstances where Two unite controllers are required in the semi-active suspension system by using the MR damper, As shown in Figure(3-10). For specific system conditions, a system controller determines the desired damping force (F_d) [90]. Then, through the second control unit, which represents the damper control, the desired force is tracked, and a voltage is produced and sent to the MR damper to produce a semi-active damping force (FMR). The damper controller's performance will depend on how well it can manage the device's nonlinear hysteretic properties. The damper and system controllers are covered in the following subsections[91].
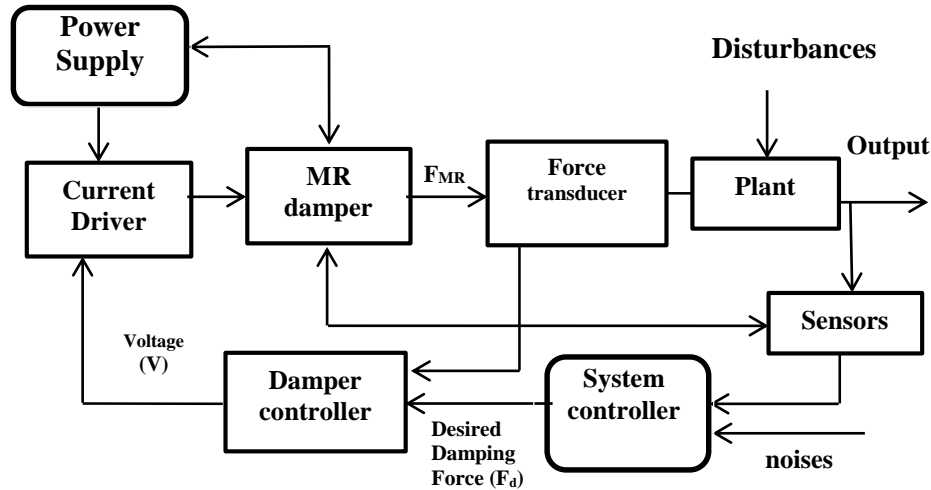
Figure 3-10: Scheme of semi-active suspension using MR damper with control unit[90].

3.6.1   Damper Controllers

The Bingham Model, which is recognised to be insufficient for MR control purposes, provides the foundation for certain techniques for managing the electrical input to the MR damper. For instance, this model was utilised in [92] to describe the damper force as Aforementioned in equation (3.7).

As a result, this formula ignores force-velocity hysteresis as well as nonlinearity with regard to mechanical inputs. The current needed to get PMR to the specified value was then calculated using a theoretical formula that links PMR to current in [92]. Since the current was increased or decreased in [93] in an effort to increase or decrease the PMR according to its desired value without comparing force feedback, the Bingham Model could only be roughly followed. Since neither of the approaches in [93] can accurately track a desired force signal, they are both ineffective. In this thesis, a specific control strategy will be selected and examined in determining the desired damping force and tracked to be converted into a variable voltage according to the type

47

of excitation and fed to the MR damper. The damper control algorithms used, which rely on simple theoretical assumptions, classify these as:

- Heaviside Step Function (HSF) control [94] [95].

- Signum Function Method (SFM) [95].

- Continuous State Control (CSC) [96].

- Inverse polynomial control [97].

- Inverse recurrent neural network (RNN) control [98].

3.6.1.1 Heaviside Step Function (HSF) Control

HSF control was first used on a car suspension system in [99] and was introduced in [100]. It operates on a "on-off" control method, with either zero or the maximum voltage applied. The following is a possible representation of the voltage selection algorithm:

$$v_i = V_{max} H\big((F_{di} - F_{MRi})F_{MRi}\big) \quad i = 1, 2 \qquad (3.38)$$

Where H is the Heaviside periodic function and V_{max} is the maximum voltage of the magnetic flux in the MR damper. The applied voltage should be constant if the MR damper delivers F_{di} necessary control force. The voltage output to the current driver be raised to its maximum level in order to raise the damper force to the required one if the total force generated by the damper F_{MRi} is lower than the controlled force F_{di}, and also the two forces are the same sign (see figure(3-10)). If not, zero is assigned as the specified voltage.

3.6.1.2 Signum Function Method (SFM)

This technique SFM, which under certain circumstances allows the supplied damper voltage to change between discrete voltage values below the maximum, is improved by the [95]. This algorithm controlled an MR damper utilised in a train's semi-active suspension system. The instruction voltage signal in these two controllers is discontinuous. Continuous voltage signalling offers more effective control, smaller power requirements, and longer damper service life [101]. The equations that describe this technique are all of the following.

$$V_{sign1} = \frac{V_{max}}{2N}\left\{\sum_{0 \le j \le N-1}\{sgn\{[F_d - (1+Kj)F_{MR}]F_{MR}\}+1\}\right\} \quad (3.39a)$$

$$V_{sign\,2} = 1 - \left[\frac{sgn(v_{sign\,1}-V_{max})+1}{2}\right] \cap \left[\frac{1-sgn(F_{MR}\dot{F}_{MR})}{2}\right] \quad (3.39b)$$

$$V_{sign} = V_{sign\,1} \times V_{sign\,2} \quad (3.40)$$

The maximum voltage to the current driver related to the magnetic field saturation in the MR fluid damper is V_{max} , and F_d and F_{MR} are the required and the controllable (measured) damping forces, respectively. Where N is an integer with $0 \le j \le$ N-1; sgn() is the signum function; $\cap$ is the logical AND; K is a small constant. v_{sign} represents the value of the voltage supplying the MR damper, which controls the damping value caused by the damper.

Using the CSC technique, a continuous voltage signal can be ordered. CSC was first employed for an ER damper in [102] before being applied for an MR damper in [96] [103], though no comparisons with different control strategies were conducted in [96] or [103]. An evaluation of the ideal damper force from

a sensor is required to feed the three different types of damper controllers (HSF, SFM, and CSC) mentioned above. For a mlulti-damper system, this sensor must be linked in series with each MRF damper, which lowers system dependability and raises system costs. Inverse polynomial and inverse RNN, each other two damper controllers mentioned above, do not need a force sensor. A repeated neural network (RNN) of the inverse dynamics of the MR damper is a more advanced technique for controlling a continual voltage signal without the necessity for a force sensor [101]. The system controller's sensors, which are already used by this controller, provide a measurement of the relative displacement throughout the damper.

3.6.2   System Controller

For the system depicted in figure (3-10), the system controller calculates the desired force needed from the MR damper to produce optimal conditions. Many system controller algorithms were created, and these may be generally categorized in accordance with the control approach used to optimize the system conditions [101]:

Direct state variable optimization

- H∞ control [103].

- Linear-Quadratic-Gaussian (LQG) control [104].

- Neural Network (NN) system control [105].

- Robust control [106].

Forcing the system to behave in a way that resembles an ideal system:

- Skyhook model and its variants [107].

- Model-reference sliding mode control [108].

In H$_\infty$ control, the controller is created by formulating an optimization problem mathematically and determining the controller gain. This method of controlling a vehicle suspension system with MR dampers has been employed in [103]. A genetic algorithm was used to create a static output feedback H$_\infty$ controller that used the body velocity and observed suspension deflection as signals received for semi-active quarter car suspension. Using time-domain numerical simulation with random stimulation, this controller was validated. Theoretical findings demonstrated that good ride comfort and vehicle stability were attained by the semi-active suspension using an MR damper controlled by static output feedback H$_\infty$ controller.

Neural networks (NN) are popular techniques for developing reliable, adaptable, and advanced control systems because of their non-linear imaging and learning capabilities. Depending on a quarter vehicle model, an adaptive system controller with a NN approach was created to operate a semi-active suspension system with an MRD [105]. Two sub-controllers made up this algorithm: a NN identity and a NN controller. The former calculates the back propagation errors for the NN controller and acts as a system controller in the semi-active system. Theoretical and experimental findings were used to investigate this algorithm. These findings demonstrated the control strategy's advantage over the passive system both the time and frequency domains.

For car suspensions employing MR dampers, LQG control can be another idea for an ideal control technique. It has been used in [104] to examine the simulated dynamic behaviour of a half-vehicle model with seat dynamics and a complete train suspension system, which have 6 and 9 degrees of freedom (DOFs) of freedom, respectively. A Linear-Quadratic Regulator and a Kalman filter were combined to create the LQG controller . The control method was

based on optimal state-feedback control gain, which was determined from the solving of the Riccati equation in algebra. The employment of MR dampers with such control technique provided the vehicle suspension system with better performance compared to a passive one, simulations in [104] demonstrated.

An alternative approach would be to compute the force so that the actual system roughly mimics the performance of an ideal system, as opposed to determining the desirable damper force on the premise of direct optimisation of the state variables. In this thesis, the Skyhook control system was relied on to improve the semi-active suspension system. In the next section, the Skyhook control system will be studied in detail and the updates made to the original system are mentioned.

3.6.2.1   Skyhook Control Method

The skyhook control is a powerful vibration control method that has a high rate of energy dissipation. The skyhook control method has been the subject of extensive study for some more than three decades. The skyhook control approach was first presented in 1974 by Karnopp et al[109]. And is still widely applied in automotive suspension applications today. The term "skyhook" refers to the notion that a passive damper might be suspended from the sky or another fictitious inertial reference point. A damping force, which is correlated to a relative velocity of the sprung mass and is in the reverse direction from that absolute velocity (Figure (3-11)).
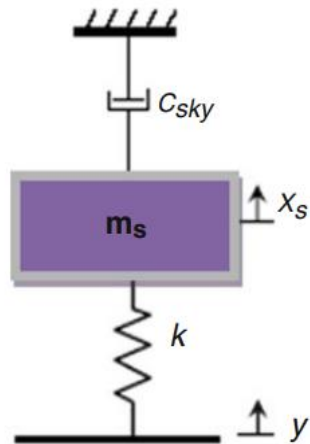
Figure 3-11: An ideal utilization for a skyhook control system[1].

The skyhook control, which has a m_s(sprung mass) connected by a damper with skyhook damping constant c_{sky} from a fictional sky (fixed ceiling), is shown in its ideal configuration in the above picture. Hence, the name "skyhook" was chosen for the control. If F_{damp} is the damping value of the skyhook damper, then the following is the optimal skyhook control law:

$$F_{damp} = -c_{sky}\dot{x}_s \qquad\qquad (3.41)$$

The ideal system for the traditional skyhook control is depicted in Figure (3-12a). That the passive damper must act as a fictional damper connected to the sprung mass at one end and a fixed point in the sky at the other. According to the experimental findings in [93], this control decreased the propagation of the sprung mass.

The skyhook controller was also employed [93] to manage the unsprung mass, where the ideal system is shown in figure (3-12b). It was referred to as "ground-hook" control in this instance. It was discovered that it lessened the un-sprung mass's transmissibility.

As in the ideal arrangement in figure (3-12c), a combination of the skyhook and ground-hook was also employed in [93]. It has been demonstrated that doing so ensures a semi-active control technique that may be gradually modified to the operating and vehicle circumstances for greater stability and comfort.
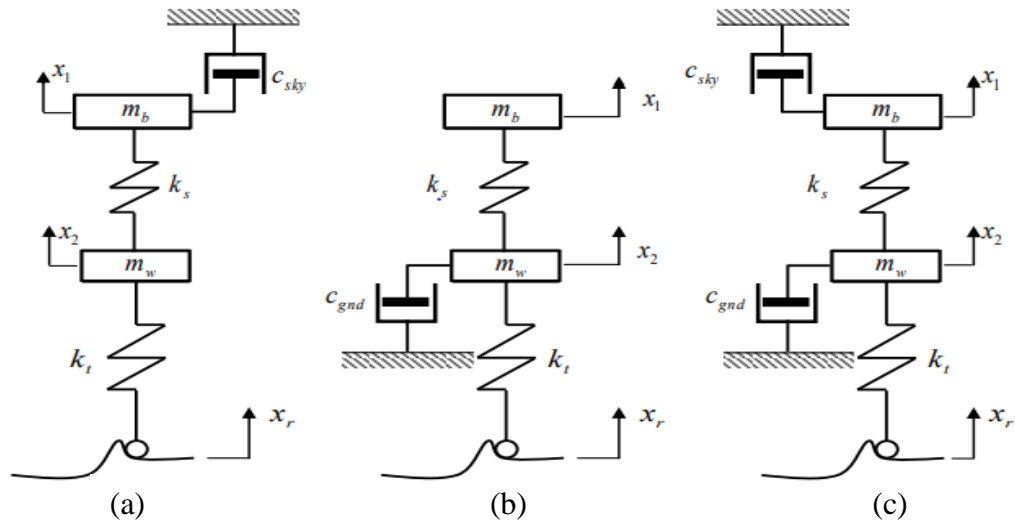
Figure 3-12: An ideal for a skyhook control system[101].

(a)Skyhook   (b) Ground-hook   (c) Combined

Three algorithms have been identified to describe the skyhook control system. The continuous skyhook control of Karnopp et al., modified skyhook control of Bessinger et al., optimal skyhook control of Nguyen et al. [103]. In this study, the modified control system of the skyhook was simulated with a quarter-car model.

3.6.2.2 Modified Skyhook Control Method

The initial skyhook control technique put out by Karnopp et al. in 1974 is changed in the skyhook control strategy described by Bessinger et al. a similar

approach was utilized in the investigation by Bakar et al. [110]. To address the issue brought on by using the classic skyhook controller, also called the water hammer, both passive and skyhook damper impacts are incorporated into the modified skyhook control method [111]. As a result, the passenger may endure unpleasant, abrupt shocks and audible noise due to the force discontinuity, known as the "water hammer" problem. The modified skyhook control algorithm's equation is given by:

$$\boldsymbol{f_d = C_{sky}[\alpha(\dot{z}_2 - \dot{z}_1)] + (1 - \alpha)\dot{z}_2} \qquad \textbf{(3.42)}$$

Where α is passive to skyhook proportion and Csky is the modified skyhook control's damping constant. The desirable force estimated in this control method is decided to be under the limit of damping forces of the intended damper. Hence the value of α is selected to be 0.5, and an ideal value of Csky is selected to be 5000.

3.7   Summary

This chapter describes the parametric models used in this thesis by studying and defining the equations for each model and specifying the versions for each model. Table (3-2) shows the selected parametric models for the simulation hysteretic behaviour of the MR damper. On the other hand, the control systems used in the simulation process were determined to control the value of the voltage supplied to the MR damper and the desired damping force. The sky hook technique was chosen to represent the control system, with the HSF technique to represent the damper control, to be applied with the Bouc-wen parametric model, chosen from among the models studied.

Table 3-2 : Parametric models were used for the simulation.

NO	Model name	Governing equation	Researchers
1	Simple Bingham model	$F_{mr} = F_c sgn(\dot{x}) + C_0\dot{x} + F_0$	Stanway et al. [72]
2	Modified Bouc–Wen model	$F_{mr} = \alpha z + c_0(\dot{x} + \dot{y}) + k_0(x - y)$ $+ k_1(x - x_0)$ $\dot{z} = -\gamma\| \dot{x} - \dot{y}\|\|z\|^{n-1}z - \beta(\dot{x} - \dot{y})\|z\|^n$ $+ A(\dot{x} - \dot{y})$ $\dot{y} = \dfrac{1}{C_0 + C_1}[\alpha z + c_0\dot{x} + k_0(x - y)]$	Spencer et al. [80]
3	Modified Dahl model	$F(t) = k_0 x(t) + c_0\dot{x} + F_d z - f_0$ $\dot{z} = \sigma\dot{x}(1 - z\,sgn(\dot{x}))$	Zhou and Qu [83]
4	Modified LuGre model II	$F(t) = \sigma_0 z + \sigma_1\dot{z} + \sigma_2\dot{x}$ $\dot{z} = \dot{x} - \sigma_0\,a_0\|\dot{x}\|z$	Sakai et al. [87][88]

Chapter Four

Simulation

Chapter 4. Simulation

4.1 Introduction

This chapter will simulate a quarter-car model with semi-active models using the MATLAB/Simulink environment. The response simulation process is considered essential in selecting the appropriate semi-active control systems in different conditions. In addition, researchers prefer to simulate the results of the system response before testing it in practice to avoid and predict problems that occur in the systems.

4.2 Road Profile Generation

The primary source of vibrations that are transferred to drivers of vehicles is road disturbances; these vibrations pass through the body of the vehicle and subsequently to the driver and passengers. Therefore, it is essential to imitate the road disturbances to examine the test suspension system and minimize those vibrations. Consequently, it was determined to employ three different input types for road disturbance to evaluate the control action. The first type represents the bump road profile in figure (4-2a), which was obtained through Simulink tools with an amplitude of 0.05m and a frequency of 2 * pi for each sine wave, with the use of transport delay1 with a value of 0.523t.(the time required for half a sine wave), which gives us two opposite sine waves As shown in figure (4-1).
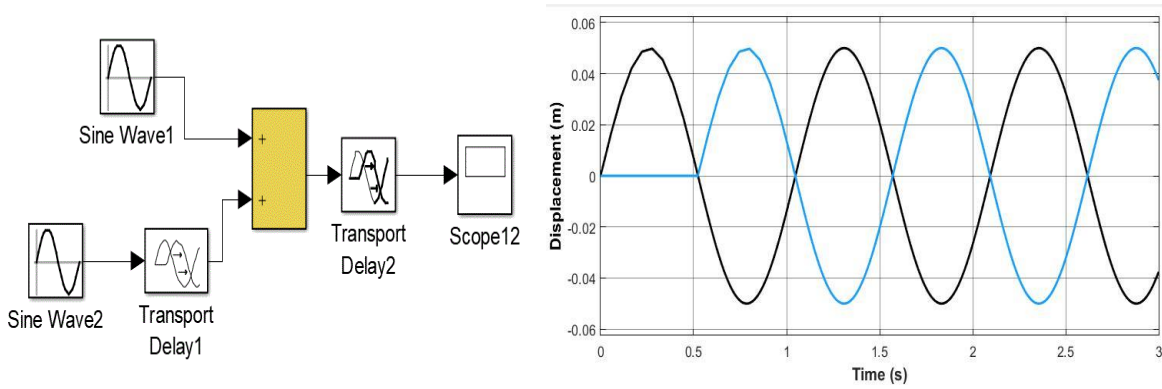
Figure 4-1: (a) Simulink of bump road profile (b) Two opposite sine waves to produce a bump road profile.

The step road profile is the second type of road disturbances, obtained from the step tool in Matlab/Simulink see figure (4-2b). Step time = 0.5t, initial value = 0m, final value = 0.05 m. A random road profile makes up the third one. The majority of road disturbance profiles in figure (4-2c), which include frequencies sensitive to human body, are random, which is the reason why the random profile was chosen. The random profile in the time domain can be produced using equation (4.1) as shown below.

$$x_r(t) = \sum_{n=1}^{N} A_n \sin(nw_0 t - \vartheta_n) \qquad (4.1)$$
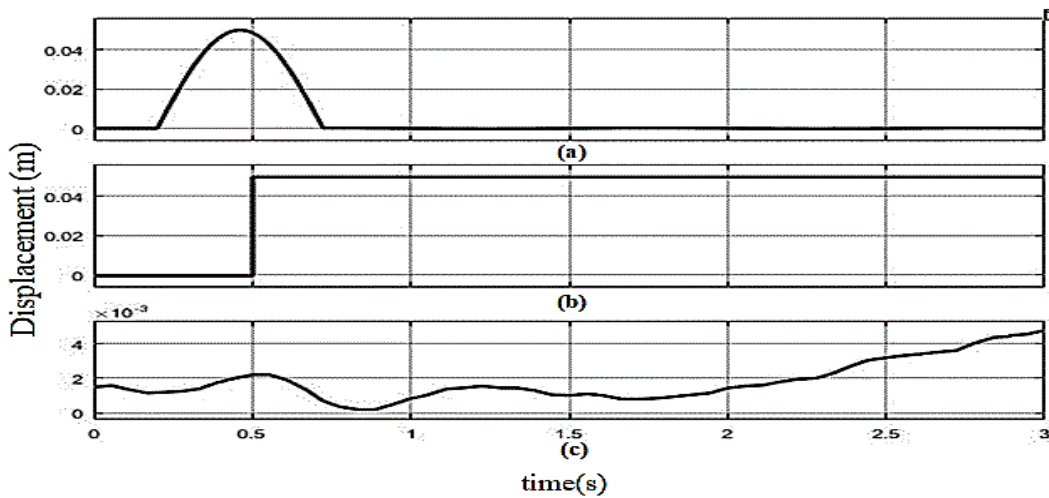
Figure 4-2: Road disturbances (a) bump (b) step (c) random road profile

59

4.3 Simulation of a Quarter-car Model

In order to simplify the simulation procedure, avoid complexity, and improve accuracy, the quarter-car suspension model is used in this study to test the vehicle's suspension system's damping effectiveness. Through simulation, the tire's mass is exposed to road disturbances simulated in the last part, and the response and effect of damping on the mass of the vehicle body are observed [111].

4.3.1   Simulation of the Passive Suspension system

The analysis of the suspension system's response using the quarter-car model with passive damping is shown in this section. The Matlab/Simulink programme was used to create the code representation of the suspension system in figure (4-3). Notably, the chapter three referred to the quarter-car model's kinematic equations look at equations (3.1 and 3.2).
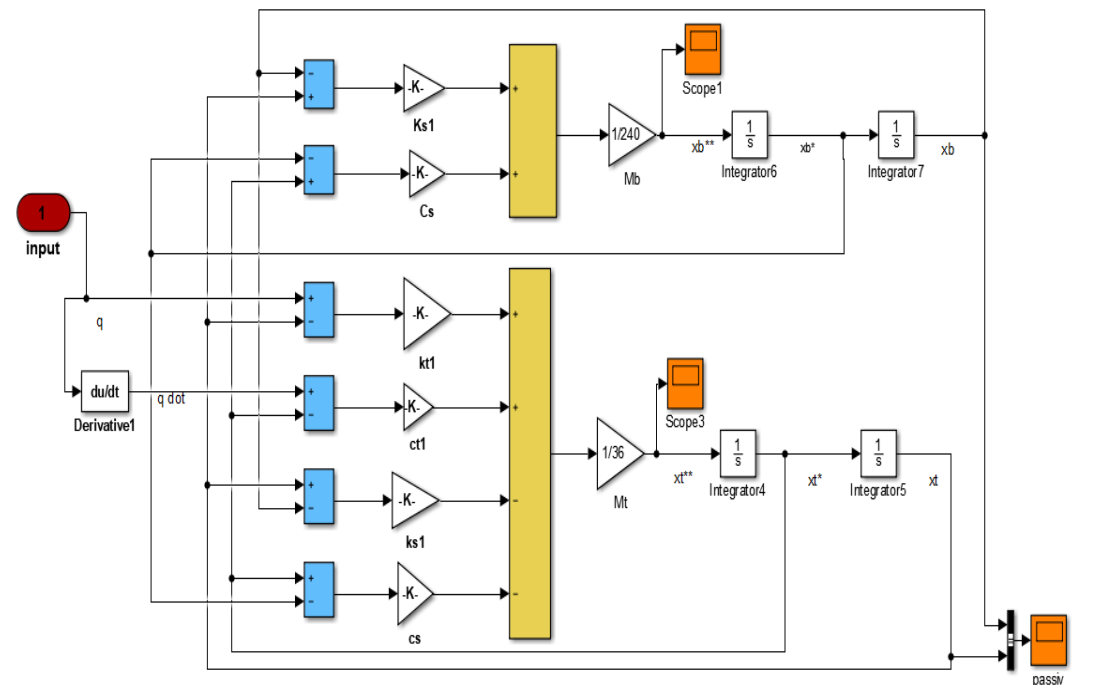
Figure 4-3: Simulink code for passive suspension system

4.3.2 Simulation of the Semi-active Suspension System

4.3.2.1 Simulation of the parametric dynamic models

After reviewing the parametric dynamic models of the MR damper in the last chapter, therefore, in this part, the parametric models that were used in this thesis (Bingham, Modified Bouc-Wen, Modified Dahl and Modified LuGre II model) will be simulated by designing a simulation code. Using a constant voltage value will be assumed in the MR damper without a damper control unit.

The Bingham model predicts the damping force resulting from the MR damper through equation (3.7), where the damping force is entered on each spring and non-spring masses with a different sign. Figure (4-4) shows the simulation code of the Bingham model in the equation of motion for the four-car model using the Simulink environment [112].
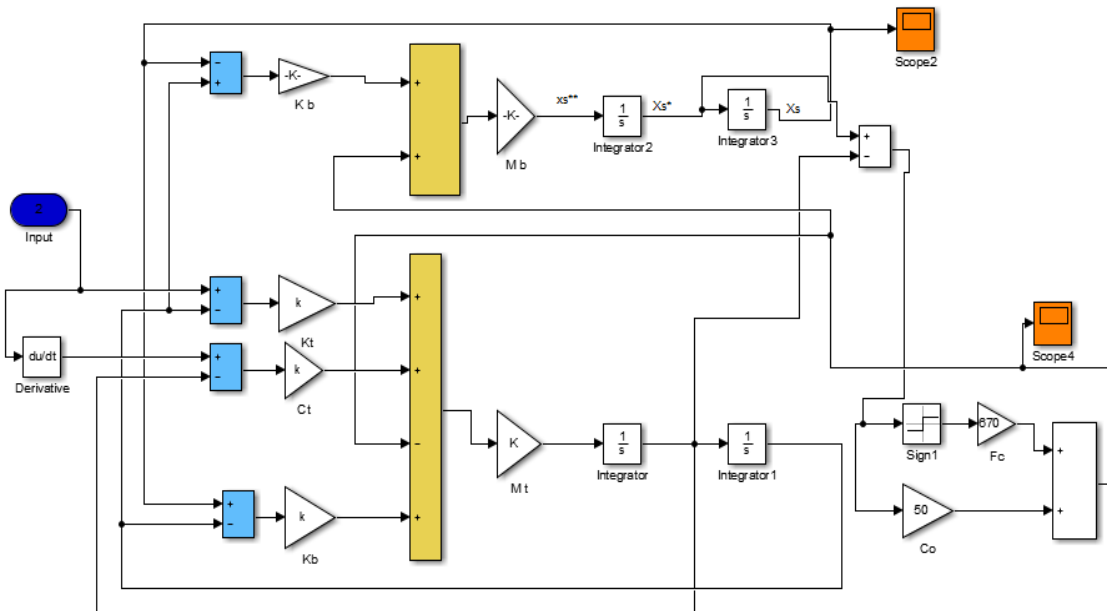
Figure 4-4: Bingham model in Simulink/MATLAB

The Bingham model does not have a direct mathematical relationship with the value of the voltage supplied to the MR damper. Therefore, to test the model changing the damping properties, it will manually control the value of the friction force f_c. Table (4-1) shows the values used in this model.

Table (4-1): The parameters for the simple Bingham model[80]

SBM	f c	C₀	f ₀
	670 N	50 N.s/cm	0

Modified Bouc–Wen model is more complex than the other models reviewed in this thesis. However, it is considered more accurate in a simulated environment where this model describes the damping force from Equation (3.15) in addition to Equation (3.16) describing the hysterical loop and Equation (3.17) representing the internal variable. In this part, these equations are simulated with the quarter-car model, as shown in Figure (4-5).

Figure 4-5: Modified Bouc-wen model in Simulink/MATLAB.

In the Modified Bouc–Wen model, equations (3.18) were used, which represent a relationship between the voltage value and the model parameters, where the values of the transactions were used in the table (4-2).

Table (4-2): Modified Bouc–Wen Model Parameter[80]

Parameter	Value	Parameter	Value
α_a	140 N/cm	k_0	46.9 N/cm
α_b	695 N/cm	k_1	5 N/cm
c_{1a}	283 N.s/cm	x_0	14 cm
c_{1b}	2.95 N.s/cm	γ	363 cm^{-2}
c_{0a}	21 N.s/cm	β	363 cm^{-2}
c_{0b}	3.5 N.s/cm	A	301
n	2	H	190 s^{-1}

The Modified Dahl model describes the hysteretic behaviour of the MR damper through equations (3.26) (3.27), where this model was simulated with a quarter car (See figure (4-6)) using the values of the model coefficients listed in Table (4-3). To change the damping characteristics, an equations (3.18a) (3.18c) is used, which represents a relationship between the voltage and the coefficients in this model. Figure (4-7) shows the Modified LuGre Model II in the MATLAB/simulation environment, as this model represents one of the simplest and most accurate models that explain the hysteretic behavior of the MR damper.
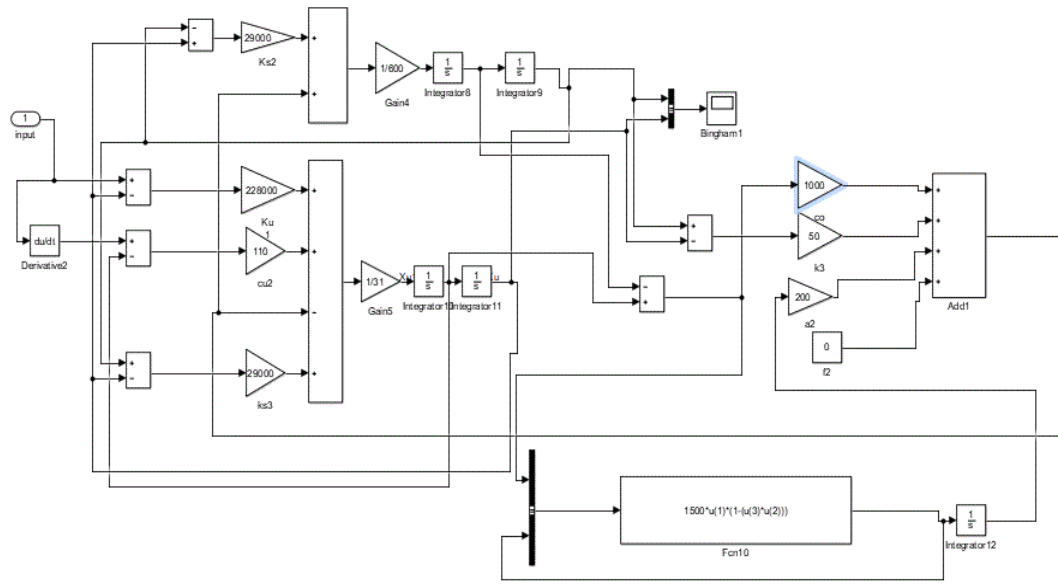
Figure 4-6: Modified Dahl Model in Simulink/MATLAB
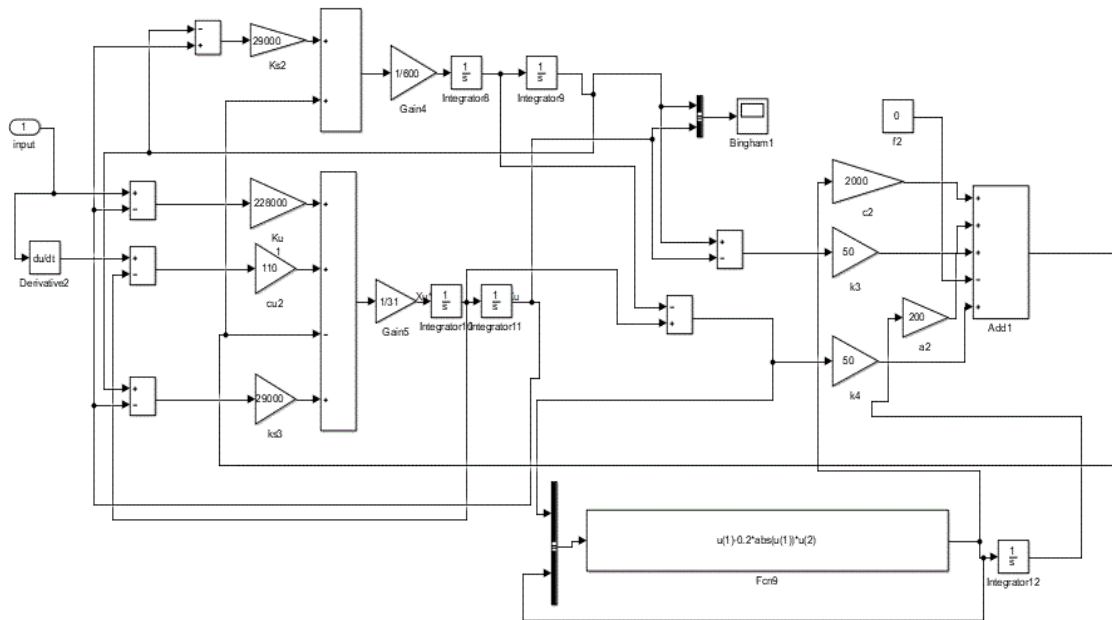
Figure 4-7: Modified LuGre Model II in Simulink/MATLAB

4.3.2.2 Simulation of Control Strategies

In order to simulate the semi-active suspension system, an appropriate control unit must be selected to achieve a realistic response in the simulation. Therefore, the Modified Skyhook technology was chosen, representing the control system described in equation (3.42) in figure (4-8), showing the simulation code for the Modified Skyhook Control Method, through which the desired damping force is predicted[113].
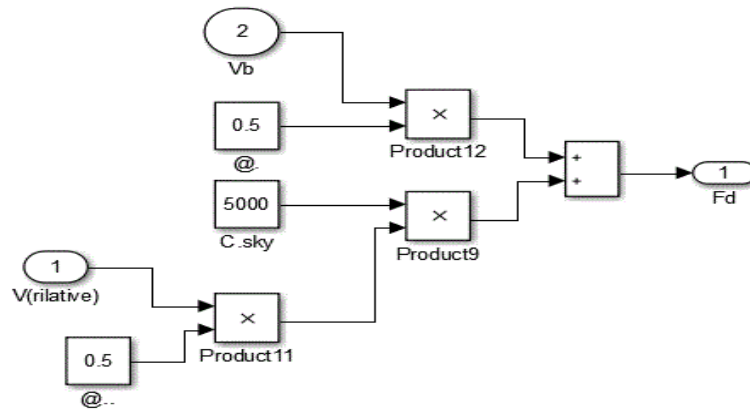
Figure 4-8: Modified Skyhook Control Method in Simulink/MATLAB

The second control unit is the damper control. In this thesis, SFM was chosen to track the damping force and send the required voltage to the MR damper. Table () showing the values used in the constants of this method. This method was introduced through equations (3.39) (3.40), which are simulated in figure (4-9).

Table (4-2): Signum Function Method (SFM)Parameter[113]

SFM	V_{max}	K	N
	12v	1	6
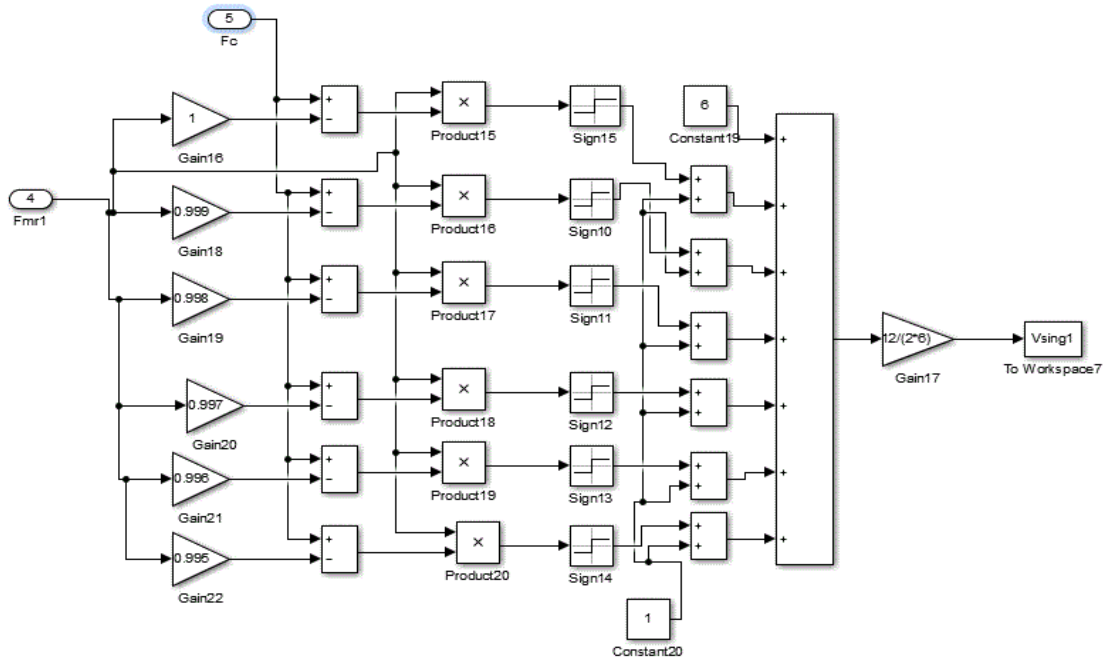
(a)
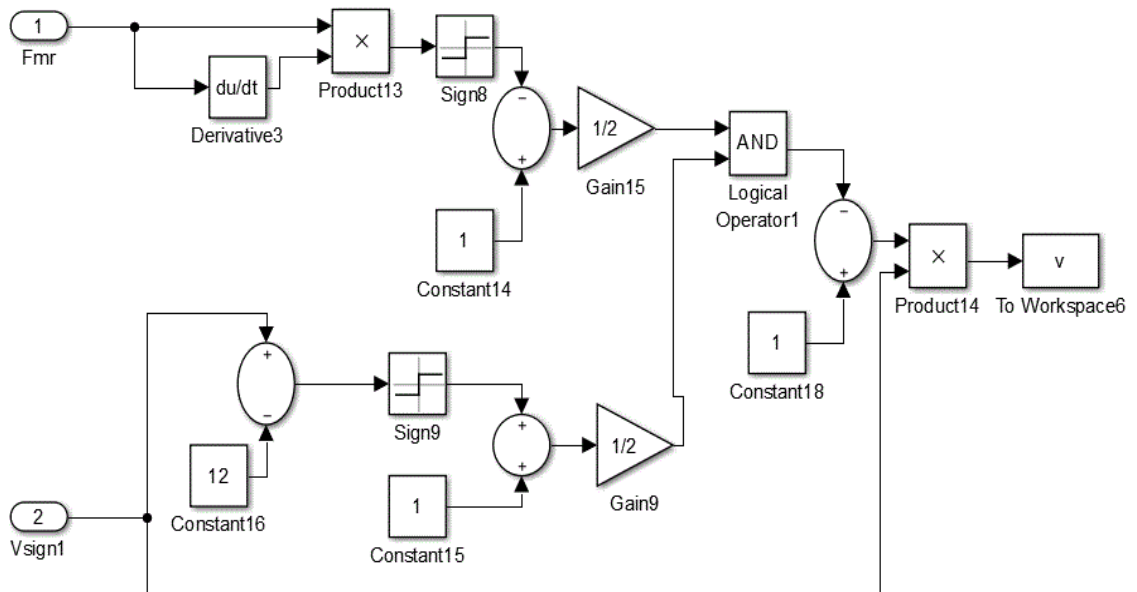
(b)

Figure 4-9: Signum Function Method (SFM) a) Vsign1 b) Vsign2 in Simulink/MATLAB

4.5 Summary

In this chapter, the four-wheel suspension system of a car using an MR damper was presented in the MATLAB/simulation environment. The codes for the parametric models that explain the MR damper's hysterical behaviour were compared in the simulation results. The response simulation process is one of the important things before the practical tests, which gives a clear picture of the type of problems facing the suspension system. In this chapter, the particular functions found in the simulation were comprehensively used to describe the equations of parametric models and the control units in the simulation process.

Chapter Five

Results and Discussion

Chapter 5. Results and Discussion

5.1   Introduction

In this chapter, the simulation results of the quarter-car suspension system will be presented after stimulating a different road inputs (step, bump). First, a comparison is made between the passive and semi-active damping systems used in the hybrid suspension system. Then, the simulation results of the semi-active models were simulated using the Matlab/Simulink environment. The following section shows the improvement in the vibration damping of the suspension system after introducing an MR damper into the system, as well as identifying the best model describing the nonlinear behaviour of MR dampers.

5.2   Response of the Semi-active Suspension System

This part aims to test the semi-active suspension system using different parametric models to explain the dynamic behaviour of the MR damper under different road profiles. The main goal is to obtain a semi-active suspension high ride comfort and reliability related to reducing vibrations caused by road excitation. After the MR damper has been tested with five different models at a constant input voltage, the best suitable models will be selected using a control unite to change the input voltage value and, according to the road, excitation to enhance the resulting damping.

5.2.1 Response of Parametric Models Without Control

After reviewing four famous parametric models in the previous chapter, the models are now simulated with the quarter-car model using only two types of road profiles. In this part of the chapter, a constant voltage value is used, which is 1.5 V equipped with the MR damper, i.e., in other words, The

damping characteristics are constant and do not change to test the parametric model's stability without a control unit.

Figure (5-1) shows the displacement of the vehicle body resulting from the road profiles, which shows the amount of damping produced for each of the passive and semi-active dampers. The displacement resulting from the bumps was reduced when using semi-active suspension models with a damping rate ranging from 10% to 30% with a damping rate at settling time ranging from 50% to 80%, depending on the model used. The damping force produced by the Semi-active damping (MRD) models caused this reduction.

(a)

(b)
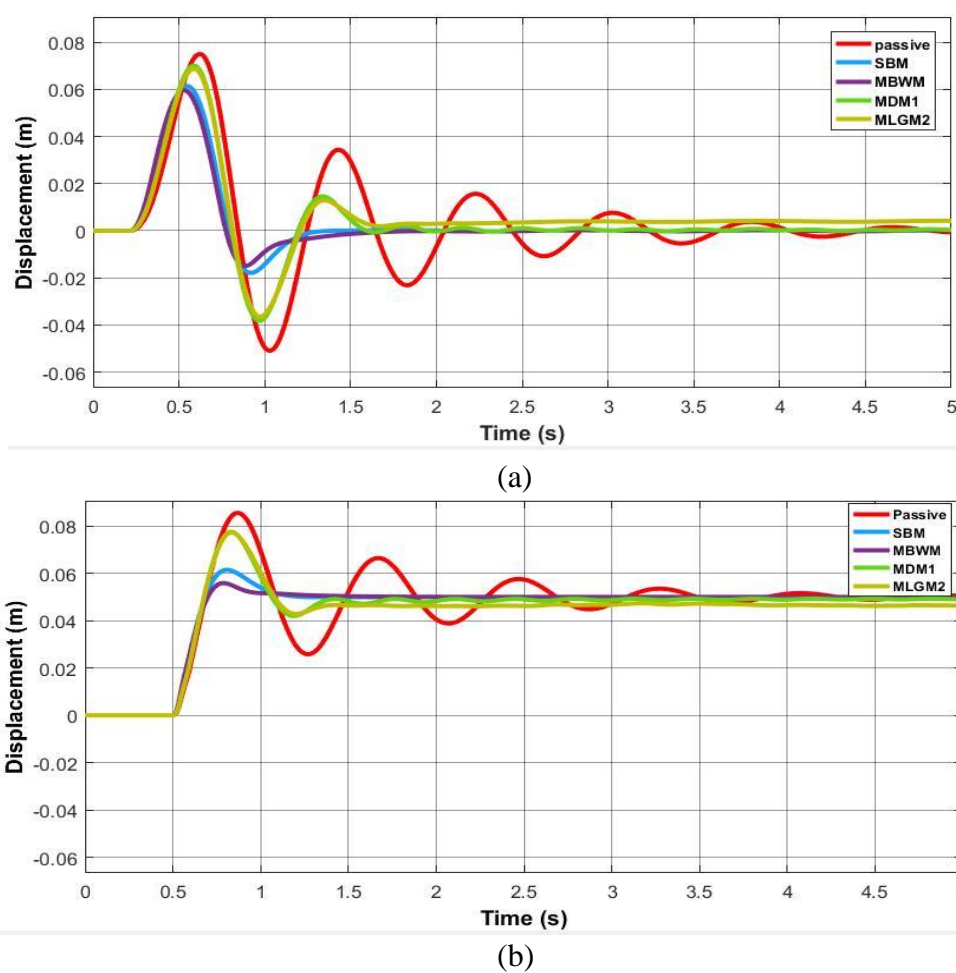
Figure 5-1: Body displacement response when exposed to road disturbances without a control unit (a) bump road profile (b) step road profile

71

Figure (5-2) shows the vehicle's body speed behaviour resulting from road bumps. The damping rate was increased in the semi-active suspension models compared to the passive suspension, as the damping rate to 10% depending on the model used to explain the behaviour of the MR damper. As a result, body stabilization time has been improved by up to 50% of the stabilization time in passive suspension.
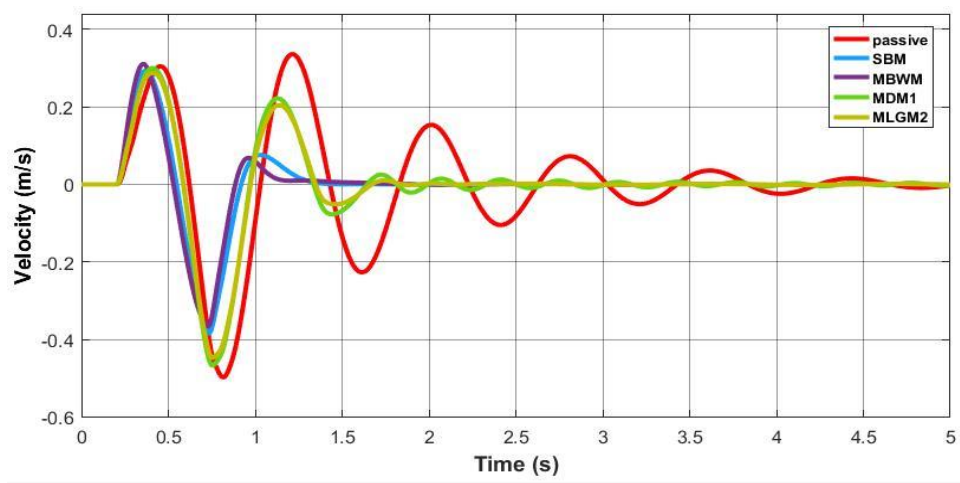
(a)
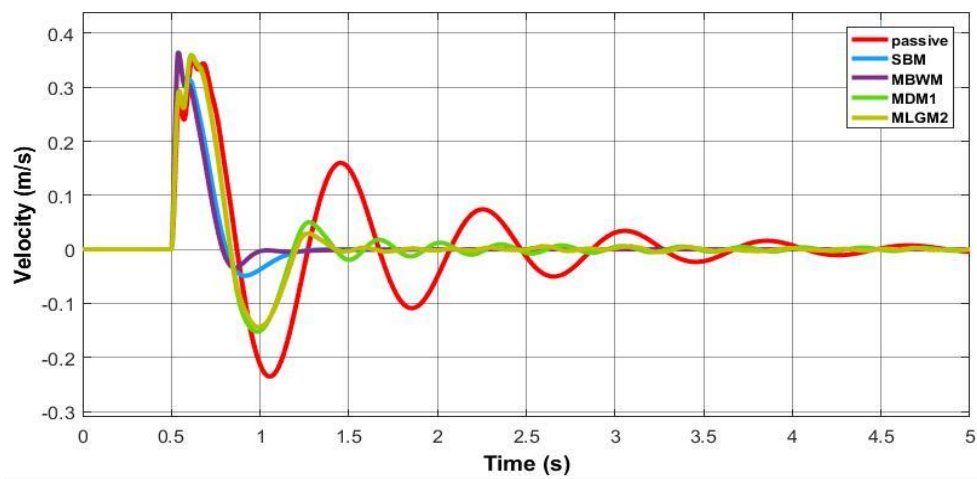
(b)

Figure 5-2: Body velocity response without a control unit

(a) bump road profile   (b) step road profile

72

Figure (5-3) shows the acceleration of the vehicle body mass resulting from road vibrations. Notice that the acceleration of the vehicle body did not decrease when using the semi-active suspension with constant voltage due to the absence of a control unit to change the damping characteristics. The body settling time is improved by 35% compared to passive suspension. Acceleration damping is one of the most critical indicators in increasing ride comfort.
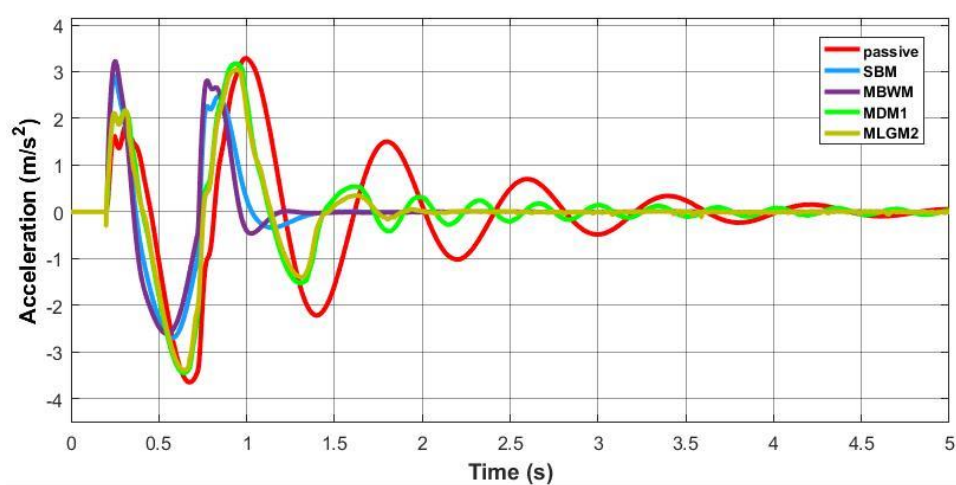
(a)
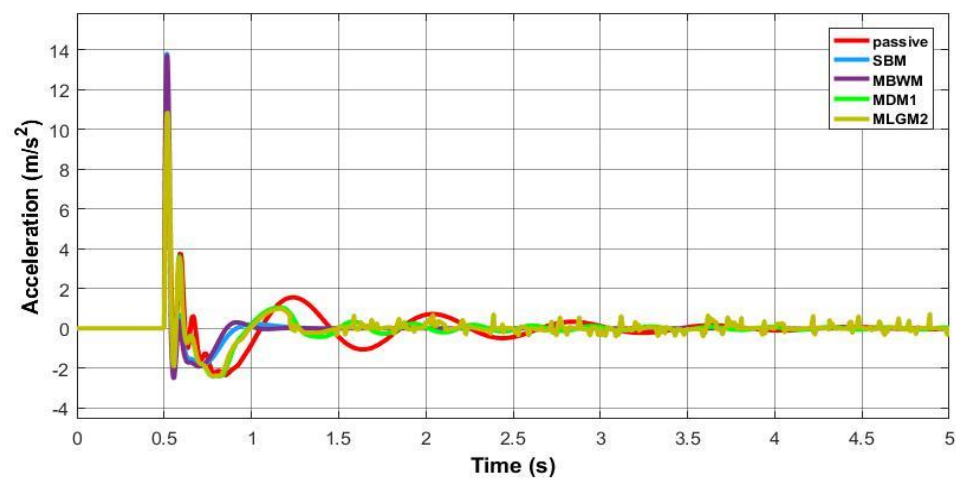
(b)

Figure 5-3: body acceleration response without control unit

(a) bump road profile   (b) step road profile

73

Figure (5-4) shows the hysteresis behaviour of the MR damper through the force-velocity (F-V) diagram using the parametric models studied in the previous chapter. Difference in the damping force produced by the MRD was found with a difference in the rheological behaviour according to the type of model used. When the value of the piston speed increases, the damping force begins to saturate, so the relationship between F-V becomes more linear and varies according to the model used. The progression of hysteresis is counterclockwise in the F-V diagram for all models, where a constant voltage of 1.5V was used with a sine wave of 2*pi frequency and 0.05m amplitude to obtain these diagrams.

(a)

(b)

(c)

(d)
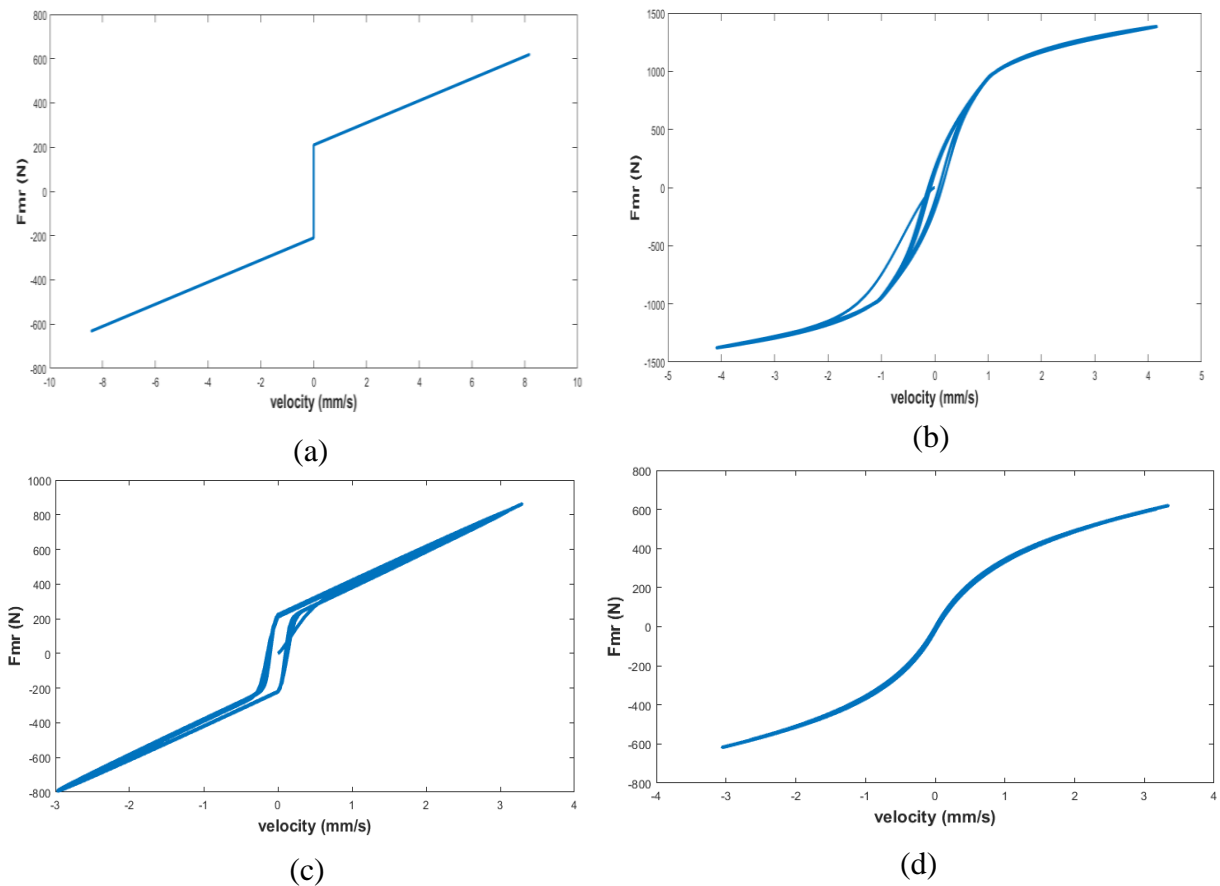
Figure 5-4: F_{MR} (N)-velocity (mm/s) in Semi-active suspension models with sine input excitation: (a) Simple Bingham Model (b) Modified Bouc–Wen model (c)Modified Dahl model (d)Modified LuGre friction model .

Figure (5-5) shows the change of the hysteresis behaviour of the MR damper in the F-V diagram after entering different voltage values as the damping force increases with the increase in the used voltage supplied to the MR damper. Where the simple Bingham model depends on the value of F_0 in controlling the voltage, the Modified Buoc-Wen model depends on the equations (3.18), which are directly related to the model factors. The Modified Dahl model depends also on the equations (3.18) to change the voltage value, and the Modified LuGre model depends on the voltage change on the α, β, γ and ε coefficients.

(a)   (b)

(c)   (d)
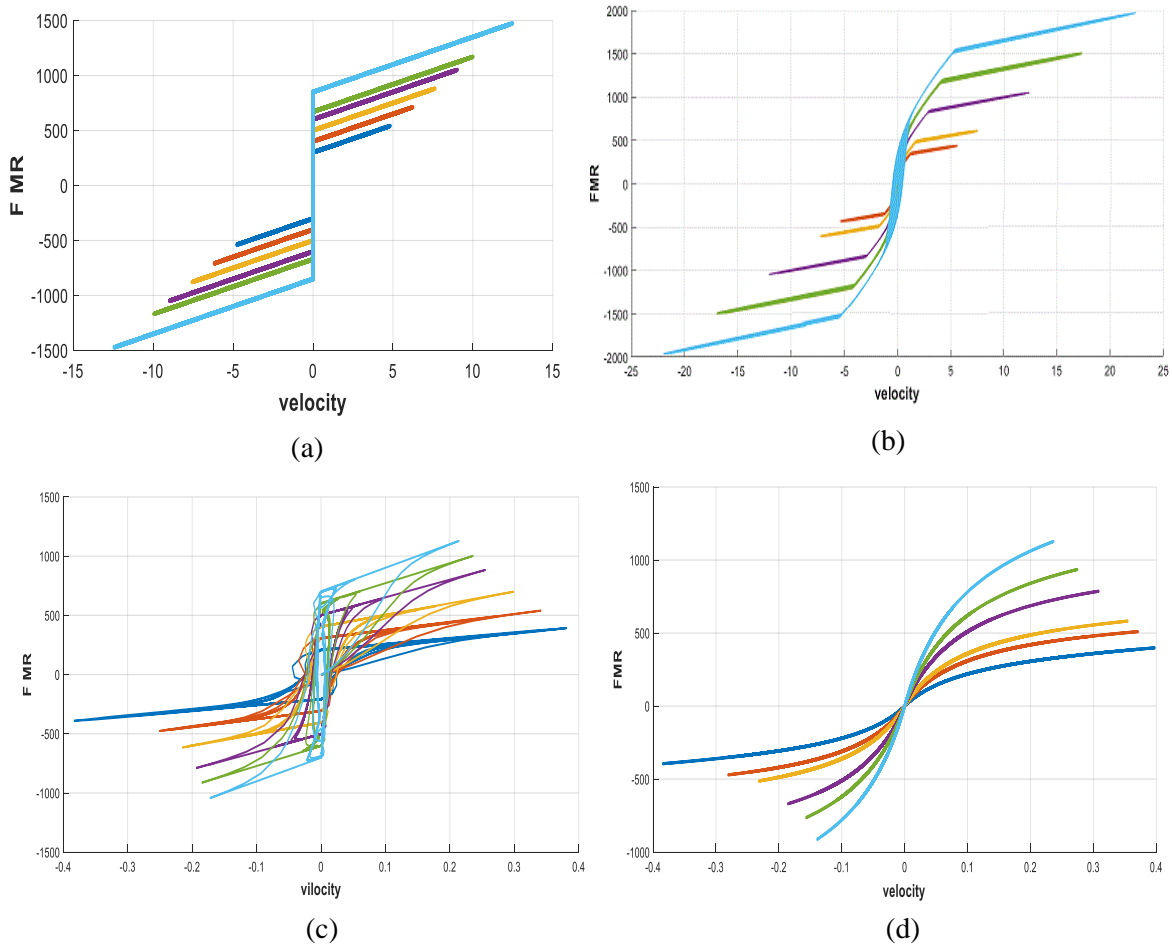
Figure 5-5: Hysterical behaviour of the MR damper between force-velocity when changing the supplied voltage: (a) SBM (b) MBWM (c) MDM1 (d) MLGM2

0 ▬▬ 0.1V ▬▬ 0.5V ▬▬ 1V ▬▬ 1.5V ▬▬ 2V ▬▬

5.2.2 Response of Parametric Models With Control

After the semi-active models were tested in the last part and compared with the passive suspension. in this part, the Modified Bouc-Wen model was selected and used with two stages of the control units in the quarter-car suspension system. The first unit is the control system, where the Modified Skyhook system was used to predict the desired damping force. In contrast, the second unit is the damper control using SFM technology, which tracks the desired damping force and gives an equivalent supplied voltage to the MR damper. Figure (5-6) shows the mass displacement damping behaviour for both passive and semi-active suspensions by using control.

(a)

(b)

(c)
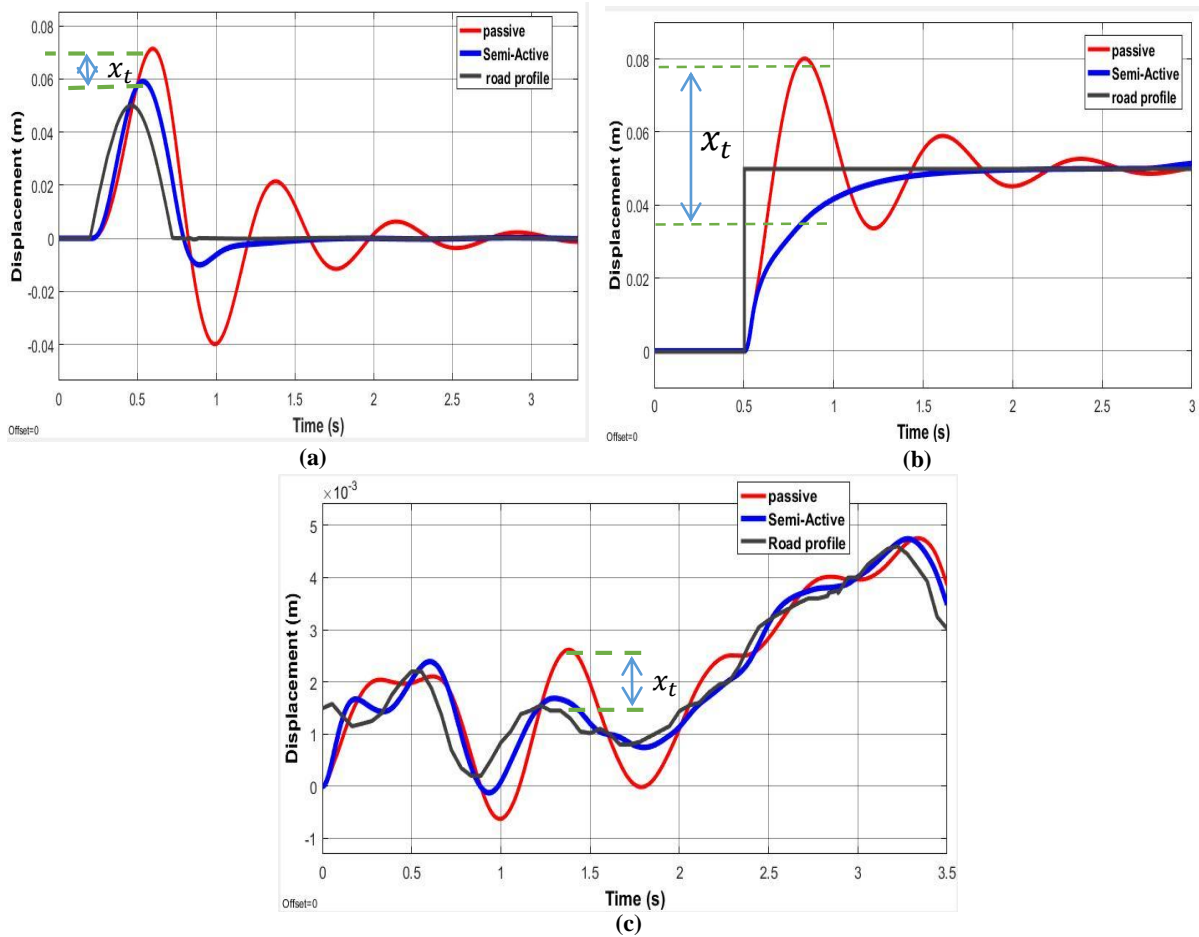
Figure 5-6:Body displacement response with the control unit (a)bump (b)step (c)random road profile

x_t is represents the improvement of damping overshoot in the mass body response when using the semi-active suspension, as it represents the difference between the highest response between the passive and semi-active suspension. The damping overshoot is 15% and 50% in the bump and step road profile and 30% at random road profile. On the other hand, the satlling time was reduced to 75%, 80% Bump and step road profile, respectively.

Figure (5-7) shows the body mass velocity response after exposure to a road profile for both passive and semi-active suspensions. The speed overshoot is damped 23%, 43% and 47% in the bump, step and random road profile , respectively. On the other hand, the mass stabilization time is improved using the semi-active suspension with the control unit.

(a)

(b)

(c)
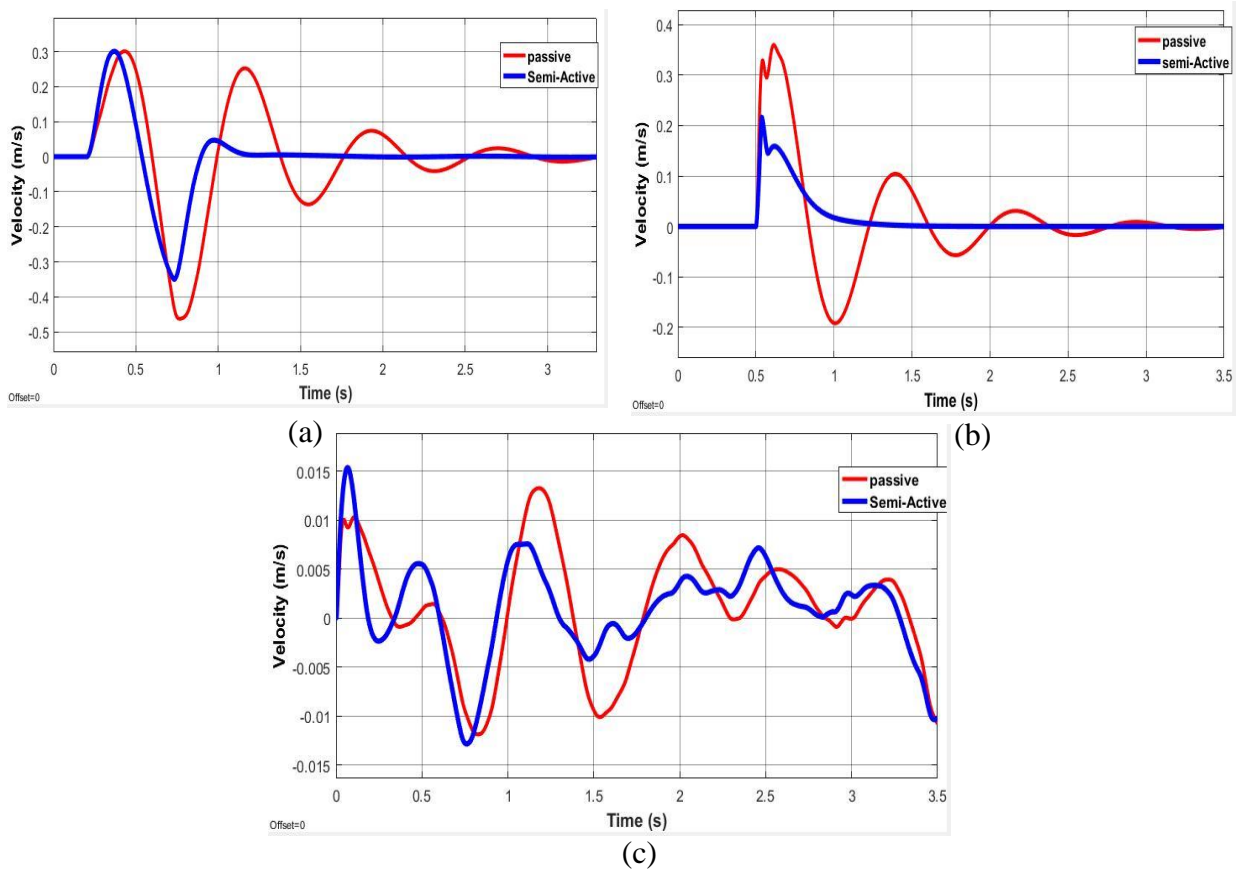
Figure 5-7:Body velocity response with the control unit (a)Bump (b)step (c) random road profile

Figure (5-8) shows the amount of damping of the mass acceleration overshoot after exposure to the road coil using the passive and semi-active suspension. 30% and 39% of damping are reached at the Bump and step road profile, respectively, with 10% of damping at random. As a result, the agitation and stabilization time of the body mass was improved.

(a)   (b)

(c)
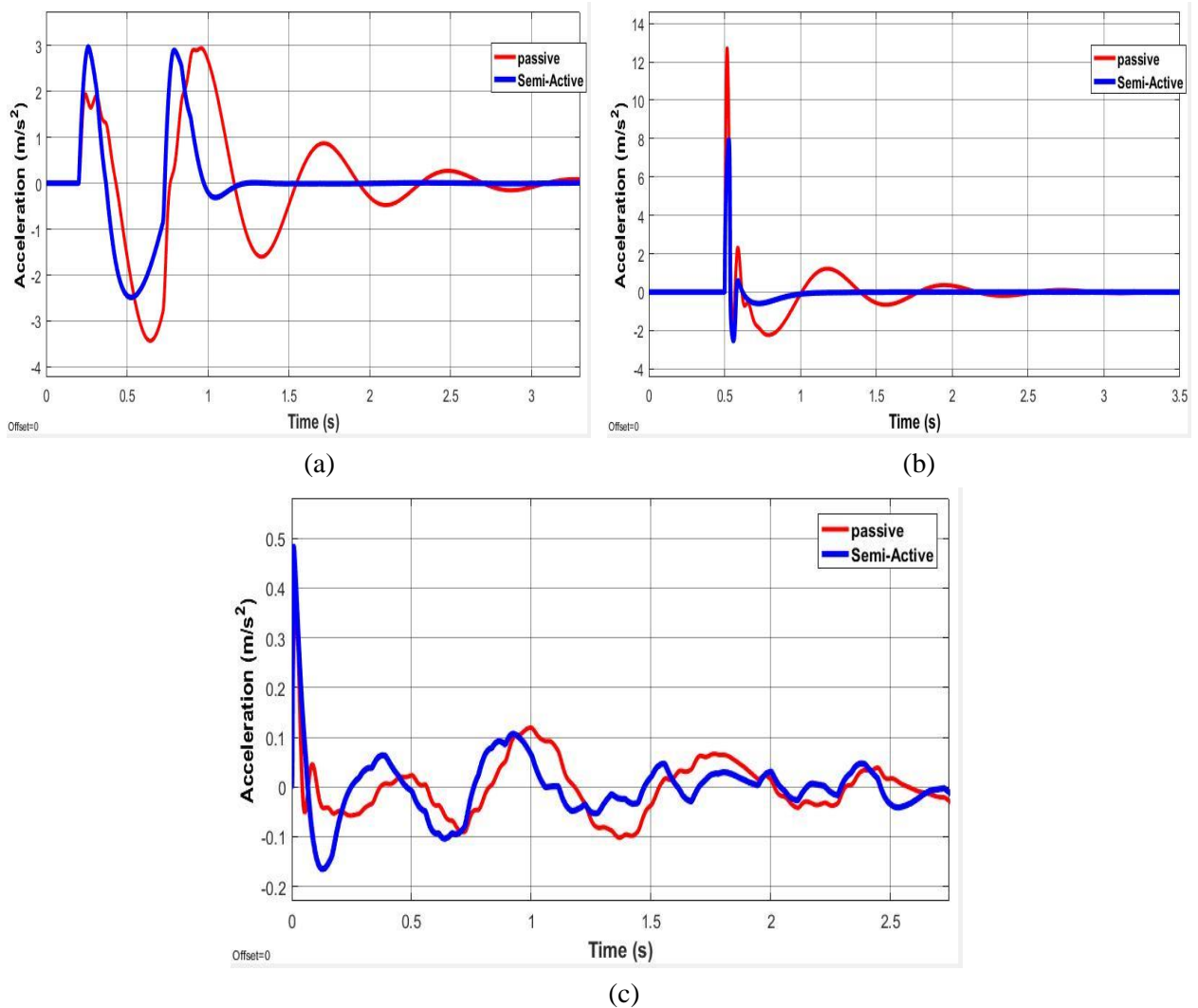
Figure 5-8:Body acceleration response with the control unit (a) Bump (b)step
(c) random road profile

After tracking the desired damping force by SFM (damper control) technology, which equips the MR damper with the required damping effort, Figure (5-9) shows the value of the required voltage according to the need of the MR damper to perform the required damping process. 12v is the maximum voltage system, and when the desired damping force approaches zero, the system voltage becomes 0V. The supplied voltage's value depends on the road profile type and its excitation capacity.

(a)

(b)

(c)
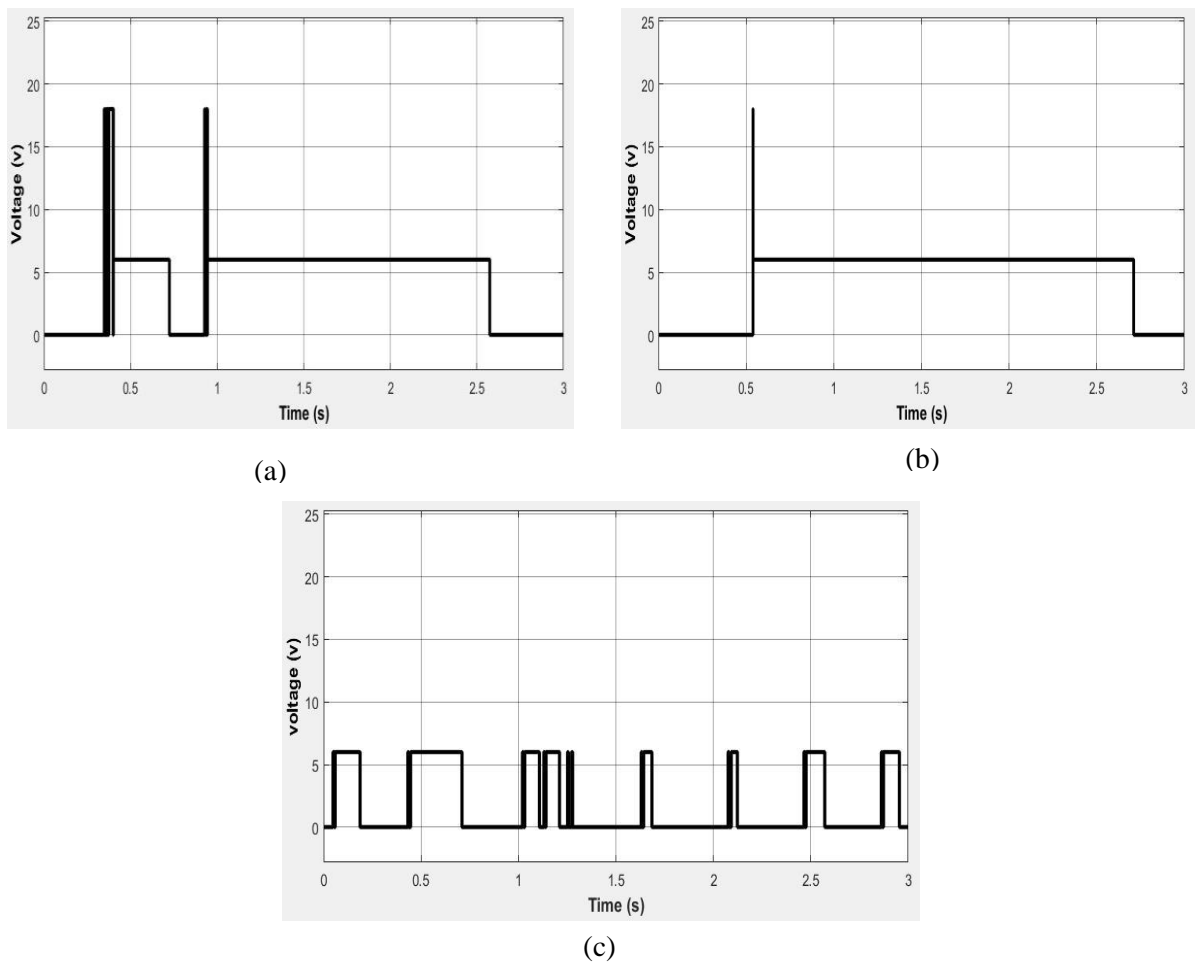
Figure 5-9: supplied voltage to MR Damper when using (a) Bump   (b) step (c) random road profile

79

Figure (5-10) shows the damping force of the MR damper using the Bouc-wen model with the Skyhook controller. Damping force varies depending on the type of road profile. The MR force is opposite to the force resulting from the road profile, which gives a negative and positive signal depending on the direction of excitation. The damping force is 1300N, 3000N and 300N at the pump, step and random road profile, respectively. These values represent the damping force when the overshoot excitation.

(a)

(b)

(c)
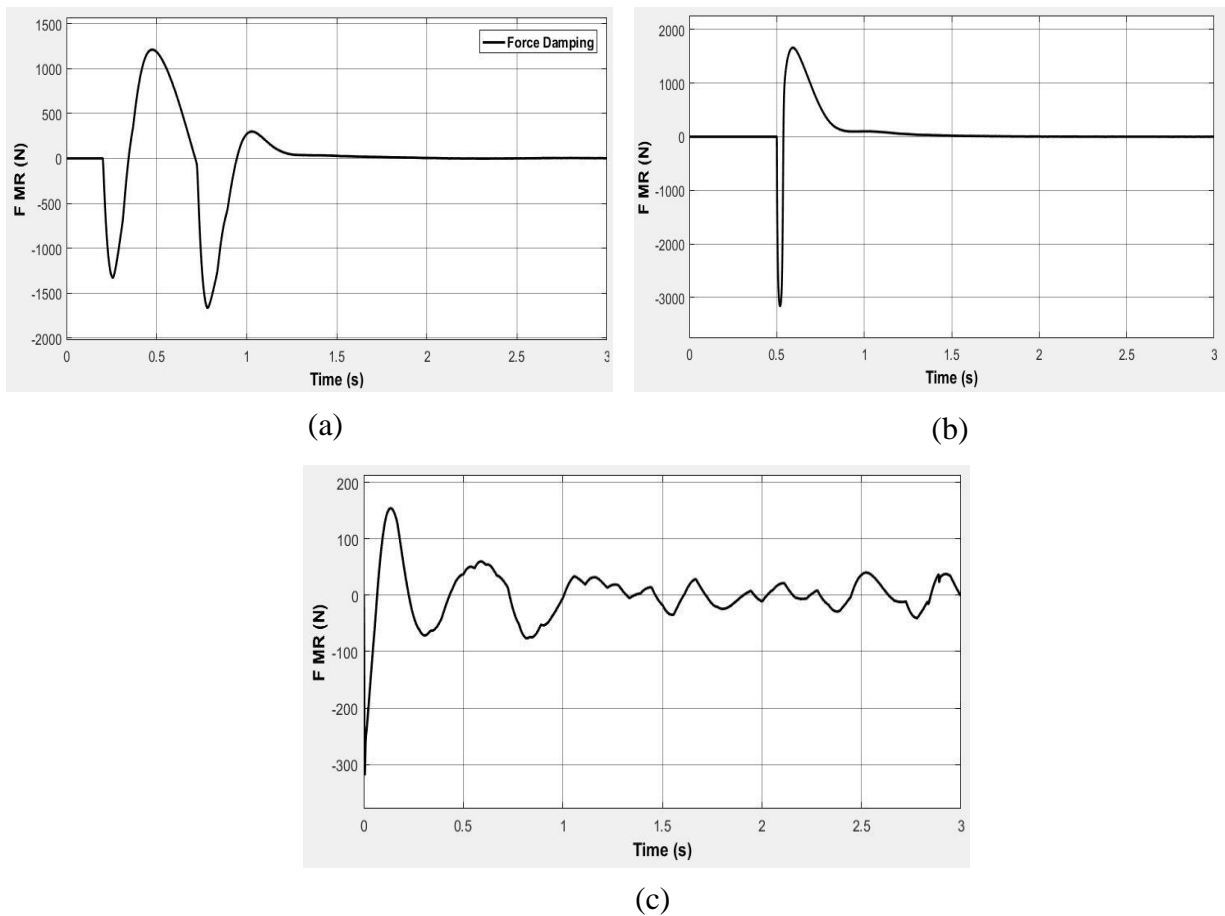
Figure 5-10: The damping force generated by the MR damper when using a control unit a) Bump   (b) step (c) random road profile

After presenting the simulation results of the quarter-car model and comparing the passive and semi-active damping, some results were summarized from the vehicle's body response to road turbulence. table(5-1) shows the steady state error values for the four parametric models. It showed a clear superiority for the SBM and MBWM models because the steady state error values in these models are close to zero, which shows the model's accuracy.

Table 5-1: steady state error values for the parametric models

Parametric model	Stady steat erorr (m)	
	Bump	Step
SBM	2×10^{-4}	≈ 0
MBWM	1×10^{-4}	≈ 0
MDM1	3×10^{-4}	-8×10^{-4}
MLGM2	4×10^{-3}	-4×10^{-3}

In table (5-2), a comparison between the passive and semi-active suspension was shown in the stabilization time of the composite body mass, as the results show the improvement in reducing the time required for stability when using the semi-active suspension. Furthermore, table (5-3) also shows the damping percentage in the overshoot value of the response simulation and for each displacement value, speed and acceleration value where the value of the damping varies according to the form of the excitement that the body of the vehicle is exposed to, as all the results that were deduced in this part were obtained manually from the figure of response to the mass body.

Table 5-2 : stabilization time between the passive and semi-active suspension

	$T_{satlling}$		
	Bump	Step	Rndom
Passive	3 s	2.5 s	-
Semi-active	1.2 s	1.5 s	-

Table 5- 3: The value of damping in semi-active suspension.

Semi-active	Displacement decrease			Velocity decrease			Acceleration decrease		
	Bump	Step	Random	Bump	Step	Random	Bump	Step	Random
Without controle	10%	30%	/	10%	10%	/	35%	30%	/
With controle	15%	50%	30%	23%	43%	47%	30%	39%	10%

5.3   Summary

In this chapter, simulation results for the passive and semi-active suspension systems were presented, and the results showed a clear improvement in the response of the vehicle body mass with an improved stability time when using the semi-active suspension.

The MR damper was tested in the quarter-car model in two cases; in the first case, four parametric differential models of the MR damper without a controller were reviewed and compared. In the second case, the Modified bouc-wen model was selected and used with the control unit (system control and damper control) to complete the work of the semi-active suspension using variable voltage on the MR damper. In both cases, the behaviour of the

hysterical MR damper was shown in the force-velocity diagram. Simulation results in the second case showed a reduction in the displacement and acceleration of the body with less stabilization time when using a control unit.

Chapter Six

Conclusion and Recommendation

Chapter 6. Conclusion and Recommendation

6.1 Conclusion

The conclusions obtained by studying semi-active suspension systems using MR damper can be summarized in this chapter. By reviewing and analyzing the most prominent parametric models that explain the non-linear behaviour of MR dampers, the following was reached:

1- The Bingham model is one of the oldest and simplest parametric models used to explain the hysterical behaviour of the MR damper. By studying the model, it was found that it was well formulated to predict hysterical behaviour with the assumption of non-zero-peston , which makes the model not capture the behaviour of the damper at speeds close to zero.

2- The Bouc-wen model is considered one of the most accurate models in explaining the hysterical behaviour of the MR damper, and it is suitable for numerical analysis. The model is used in many practical studies of the MR damper by adding semi-active control units.

3- To use the MR damper in the semi-active suspension, a control unit consisting of two parts must be used to complete the work of the semi-active suspension in addition to the MR damper models .

4- The Skyhook control system is considered one of the simplest systems used in numerical simulation and has good acceptability in estimating the desired damping force.

5- After using three types of road turbulence on the semi-active quarter car model, the displacement damping ratio was reached, ranging from 30% to 50%, while reducing the stabilization time of the body to about 60%. As a result, the mass acceleration resulting from road turbulence was damped to about 35% less than the acceleration in a passive suspension.

6.2 Recommendation

The recommendations listed below are offered as ideas for future work based on the work completed for this thesis.

1- It is possible to extensively compare parametric and non-parametric models using auxiliary programs for numerical reasoning.

2- It is possible to manufacture a quarter car model with the use of an MR damper and obtain practical results and compare them with the analytical results to reach the most accurate parametric model.

3- Using other control systems to predict the desired damping force may be useful. Examples include PID, LQR, Fuzzy and other semi-active control systems and can also be compared.

References

[1] Kashem, S., Nagarajah, R. and Ektesabi, M., 2018. Vehicle Suspension System. In Vehicle Suspension Systems and Electromagnetic Dampers (pp. 23-37). Springer, Singapore.

[2] S. S. Jadhav and A. PShrotri,. 'Suspension system with broad classification and various models: a review.' International Journal of Advanced Technology in Engineering and Science.Vol. No4, Isseu,No 2,Fabruary 2016."

[3] Al-Zughaibi, A. and Davies, H.C., 2015. Controller design for active suspension system of ¼ car with unknown mass and time-delay. World Academy of Science, Engineering and Technology International Journal of Mechanical, Aerospace, Industrial, Mechatronic and Manufacturing Engineering, 9(8), pp.1176-1181.

[4] Dowds, P. and O'Dwyer, A., 2005. Modelling and control of a suspension system for vehicle applications

[5] Karnopp, D., Crosby, M.J. and Harwood, R.A., 1974. Vibration control using semi-active force generators.

[6] Suda, Y., Shiiba, T., Hio, K., Kawamoto, Y., Kondo, T. and Yamagata, H., 2004. Study on electromagnetic damper for automobiles with nonlinear damping force characteristics (road test and theoretical analysis). Vehicle System Dynamics, 41(SUPPL.), pp.637-646.

[7] https://www.lord.com/products-and-solutions/active-vibration-control/industrial-suspension-systems/magneto-rheological-mr-fluid

[8] Rabinow, J., 1948. The magnetic fluid clutch. Electrical Engineering, 67(12), pp.1167-1167.

[9] Vinod, S., John, R. and Philip, J., 2016. Magnetorheological properties of sodium sulphonate capped electrolytic iron based MR fluid: a comparison with CI based MR fluid. Smart Materials and Structures, 26(2), p.025003.

[10] Yao, G.Z., Yap, F.F., Chen, G., Li, W. and Yeo, S.H., 2002. MR damper and its application for semi-active con trol of vehicle suspension system. Mechatronics, 12(7), pp.963-973.

[11] Zhu, X., Jing, X. and Cheng, L., 2012. Magnetorheological fluid dampers: a review on structure design and analysis. Journal of intelligent material systems and structures, 23(8), pp.839-873.

[12] Carlson, J.D., Catanzarite, D.M. and St. Clair, K.A., 1996. Commercial magneto-rheological fluid devices. International Journal of Modern Physics B, 10(23n24), pp.2857-2865.

[13] Lajqi, S. and Pehan, S., 2012. Designs and optimizations of active and semi-active non-linear suspension systems for a terrain vehicle. Strojniški vestnik-journal of mechanical engineering, 58(12), pp.732-743.

[14] Mitra, A.C., Patil, M.V. and Banerjee, N., 2015. Optimization of vehicle suspension parameters for ride comfort based on RSM. Journal of The Institution of Engineers (India): Series C, 96(2), pp.165-173.

[15] Al-Zughaibi, A.I., 2018. Experimental and analytical investigations of friction at lubricant bearings in passive suspension systems. Nonlinear Dynamics, 94(2), pp.1227-1242.

[16]   Dowds, P. and O'Dwyer, A., 2005. Modelling and control of a suspension system for vehicle applications.

[17] Sam, Y.M., Osman, J.H. and Ghani, M.R.A., 2004. A class of proportional-integral sliding mode control with application to active suspension system. Systems & control letters, 51(3-4), pp.217-223.

[18]   Divekar, A.A. and Mahajan, B.D., 2016, May. Analytical modeling and self-Tuned fuzzy-PID logic based control for quarter Car Suspension System using simulink. In 2016 IEEE International Conference on Recent Trends in Electronics, Information & Communication Technology (RTEICT) (pp. 267-271). IEEE.

[19]   Kilicaslan, S., 2018. Control of active suspension system considering nonlinear actuator dynamics. Nonlinear dynamics, 91(2), pp.1383-1394.

[20]   Sellami, A. and Zanzouri, N., 2017, March. Fault diagnosis of a vehicular active suspension system by Luenberger observer using bond graph approach. In 2017 International Conference on Green Energy Conversion Systems (GECS) (pp. 1-8). IEEE.

[21]   Lv, H., Sun, Q. and Zhang, W.J., 2021, September. A Comparative Study of Four Parametric Hysteresis Models for Magnetorheological Dampers. In Actuators (Vol. 10, No. 10, p. 257). MDPI.

[22] Zhang, T. and Ren, Z., 2022, April. Research on the arctangent function mechanical model of magneto-rheological damper. In 2nd International Conference on Mechanical, Electronics, and Electrical and Automation Control (METMS 2022) (Vol. 12244, pp. 1063-1069). SPIE.

[23]   Tu, F., Yang, Q., He, C. and Wang, L., 2012. Experimental study and design on automobile suspension made of magneto-rheological damper. Energy Procedia, 16, pp.417-425.

[24] Hingane, Amit A., et al. ,2013.Analysis of semi active suspension system with bingham model subjected to random road excitation using MATLAB/Simulink." IOSR Journal of Mechanical and Civil Engineering 3.1 ,pp 01-06.

[25] Şahin, İ., Engin, T. and Çeşmeci, Ş., 2010. Comparison of some existing parametric models for magnetorheological fluid dampers. Smart materials and structures, 19(3), p.035012.

[26] Choi, S., Lee, S., & Park, Y. 2001. A hysteresis model for the field-dependent damping force of a magnetorheological damper. Journal of Sound and Vibration, vol.245, pp375-383.

[27] Metered, H., 2012. Application of nonparametric magnetorheological damper model in vehicle semi-active suspension system. SAE International Journal of Passenger Cars-Mechanical Systems, 5(2012-01-0977), pp.715-726.

[28] Du, H., Sze, K.Y. and Lam, J., 2005. Semi-active H∞ control of vehicle suspension with magneto-rheological dampers. Journal of sound and vibration, 283(3-5), pp.981-996.

[29] Elsawaf, A., Metered, H. and Abdelhamid, A., 2019. Minimizing Power Consumption of Fully Active Vehicle Suspension System Using Combined Multi-Objective Particle Swarm Optimization (No. 2019-01-5077). SAE Technical Paper.

[30] Rao, K.D., 2014. Modeling, simulation and control of semi active suspension system for automobiles under matlab simulink using pid controller. IFAC Proceedings Volumes, 47(1), pp.827-831.

[31] Shojaei, A., Metered, H., Shojaei, S. and Olutunde Oyadiji, S., 2013. Theoretical and Experimental Investigation of Magneto-Rheological

Damper based Semi-Active Suspension Systems. International Journal of Vehicle Structures & Systems (IJVSS), 5.

[32] Carlson, J.D. and Jolly, M.R., 2000. MR fluid, foam and elastomer devices. mechatronics, 10(4-5), pp.555-569.

[33] Zhang, H., Winner, H., & Li, W. 2009. Comparison between Skyhook and Minimax Control Strategies for Semi-active Suspension System. World Academy of Science, Engineering and Technology, International Journal of Mechanical, Aerospace, Industrial, Mechatronic and Manufacturing Engineering, 3, pp.845-848.

[34] Rankin, P.J., Ginder, J.M. and Klingenberg, D.J., 1998. Electro-and magneto-rheology. Current opinion in colloid & interface science, 3(4), pp.373-381.

[35] De Vicente, J., Klingenberg, D.J. and Hidalgo-Alvarez, R., 2011. Magnetorheological fluids: a review. Soft matter, 7(8), pp.3701-3710.

[36] Carlson, J.D. and Jolly, M.R., 2000. MR fluid, foam and elastomer devices. mechatronics, 10(4-5), pp.555-569.

[37] Phillips, R.W., 1969. Engineering applications of fluids with a variable yield stress. University of California, Berkeley.

[38] Choi, Y.T., Cho, J.U., Choi, S.B. and Wereley, N.M., 2005. Constitutive models of electrorheological and magnetorheological fluids using viscometers. Smart materials and structures, 14(5), p.1025.

[39] Wang, X. and Gordaninejad, F., 1999. Flow analysis of field-controllable, electro-and magneto-rheological fluids using Herschel-Bulkley model. Journal of Intelligent Material Systems and Structures, 10(8), pp.601-608.

[40] Stanway, R., Sproston, J.L. and El-Wahed, A.K., 1996. Applications of electro-rheological fluids in vibration control: a survey. Smart Materials and Structures, 5(4), p.464.

[41] Goncalves, F.D., Koo, J.H. and Ahmadian, M., 2006. A review of the state of the art in magnetorheological fluid technologies--Part I: MR fluid and MR fluid models. The Shock and Vibration Digest, 38(3), pp.203-220.

[42] Wilson, S.D.R., 1993. Squeezing flow of a Bingham material. Journal of Non-Newtonian Fluid Mechanics, 47, pp.211-219.

[43] Wilson, S.D.R., 1993. Squeezing flow of a Bingham material. Journal of Non-Newtonian Fluid Mechanics, 47, pp.211-219.

[44] Ahamed, R., Ferdaus, M.M. and Li, Y., 2016. Advancement in energy harvesting magneto-rheological fluid damper: A review. Korea-Australia Rheology Journal, 28(4), pp.355-379.

[45] Crivellaro, C. and Donha, D.C., 2008. Discrete-time dynamic model of a magneto-rheological damper for semi-active control design. In ABCM Symposium Series in Mechatronics (Vol. 3, pp. 27-36).

[46] Spencer Jr, B.F. and Nagarajaiah, S., 2003. State of the art of structural control. Journal of structural engineering, 129(7), pp.845-856.

[47] Lai, C.Y. and Liao, W.H., 2002. Vibration control of a suspension system via a magnetorheological fluid damper. Journal of Vibration and Control, 8(4), pp.527-547.

[48] Wang, D.H. and Liao, W.H., 2009. Semi-active suspension systems for railway vehicles using magnetorheological dampers. Part I: system integration and modelling. Vehicle System Dynamics, 47(11), pp.1305-1325.

[49] Soltane, S., Montassar, S., Ben Mekki, O. and El Fatmi, R., 2015. A hysteretic Bingham model for MR dampers to control cable vibrations. Journal of Mechanics of Materials and Structures, 10(2), pp.195-206.

[50] Boada, M.J.L., Calvo, J.A., Boada, B.L. and Díaz, V., 2011. Modeling of a magnetorheological damper by recursive lazy learning. International Journal of Non-Linear Mechanics, 46(3), pp.479-485.

[51] Arias-Montiel, M., Florean-Aquino, K.H., Francisco-Agustin, E., Pinon-Lopez, D.M., Santos-Ortiz, R.J. and Santiago-Marcial, B.A., 2015, November. Experimental characterization of a magnetorheological damper by a polynomial model. In 2015 International Conference on Mechatronics, Electronics and Automotive Engineering (ICMEAE) (pp. 128-133). IEEE.

[52] Kim, K.J., Lee, C.W. and Koo, J.H., 2008. Design and modeling of semi-active squeeze film dampers using magneto-rheological fluids. Smart Materials and Structures, 17(3), p.035006.

[53] Schurter, K.C. and Roschke, P.N., 2000, May. Fuzzy modeling of a magnetorheological damper using ANFIS. In Ninth IEEE International Conference on Fuzzy Systems. FUZZ-IEEE 2000 (Cat. No. 00CH37063) (Vol. 1, pp. 122-127). IEEE.

[54] Koga, K. and Sano, A., 2006, June. Query-based approach to prediction of MR damper force with application to vibration control. In 2006 American Control Conference (pp. 7-pp). IEEE.

[55] Chang, C.C. and Roschke, P., 1998. Neural network modeling of a magnetorheological damper. Journal of intelligent material systems and structures, 9(9), pp.755-764.

[56] Du, H., Lam, J. and Zhang, N., 2006. Modelling of a magneto-rheological damper by evolving radial basis function networks. Engineering Applications of Artificial Intelligence, 19(8), pp.869-881.

[57] Jin, G., Sain, M.K., Pham, K.D., Billie, F.S. and Ramallo, J.C., 2001, June. Modeling MR-dampers: a nonlinear blackbox approach. In Proceedings of the 2001 American Control Conference.(Cat. No. 01CH37148) (Vol. 1, pp. 429-434). IEEE.

[58] Savaresi, S.M., Bittanti, S. and Montiglio, M., 2005. Identification of semi-physical and black-box non-linear models: the case of MR-dampers for vehicles control. Automatica, 41(1), pp.113-127.

[59] Jin, G., Sain, M.K. and Spencer, B.E., 2005. Nonlinear blackbox modeling of MR-dampers for civil structural control. IEEE Transactions on Control Systems Technology, 13(3), pp.345-355.

[60] Wang, D.H. and Liao, W.H., 2011. Magnetorheological fluid dampers: a review of parametric modelling. Smart materials and structures, 20(2), p.023001.

[61] Jimnez, R. and Alvarez, L., 2002, December. Real time identification of structures with magnetorheological dampers. In Proceedings of the 41st IEEE Conference on Decision and Control, 2002. (Vol. 1, pp. 1017-1022). IEEE.

[62] Jimnez, R. and Alvarez, L., 2002, December. Real time identification of structures with magnetorheological dampers. In Proceedings of the 41st IEEE Conference on Decision and Control, 2002. (Vol. 1, pp. 1017-1022). IEEE.

[63] Oh, H.U., 2004. Experimental demonstration of an improved magneto-rheological fluid damper for suppression of vibration of a space flexible structure. Smart materials and structures, 13(5), p.1238.

[64] Şahin, İ., Engin, T. and Çeşmeci, Ş., 2010. Comparison of some existing parametric models for magnetorheological fluid dampers. Smart materials and structures, 19(3), p.035012.

[65] Dominguez, A., Sedaghati, R. and Stiharu, I., 2004. Modelling the hysteresis phenomenon of magnetorheological dampers. Smart Materials and Structures, 13(6), p.1351.

[66] Dominguez, A., Sedaghati, R. and Stiharu, I., 2008. Modeling and application of MR dampers in semi-adaptive structures. Computers & structures, 86(3-5), pp.407-415.

[67] Ikhouane, F. and Dyke, S.J., 2007. Modeling and identification of a shear mode magnetorheological damper. Smart Materials and Structures, 16(3), p.605.

[68] Kwok, N.M., Ha, Q.P., Nguyen, T.H., Li, J. and Samali, B., 2006. A novel hysteretic model for magnetorheological fluid dampers and parameter identification using particle swarm optimization. Sensors and Actuators A: Physical, 132(2), pp.441-451.

[69] Hu, W. and Wereley, N.M., 2008. Hybrid magnetorheological fluid–elastomeric lag dampers for helicopter stability augmentation. Smart Materials and Structures, 17(4), p.045021.

[70] Ma, X.Q., Rakheja, S. and Su, C.Y., 2007. Development and relative assessments of models for characterizing the current dependent hysteresis properties of magnetorheological fluid dampers. Journal of intelligent material systems and structures, 18(5), pp.487-502.

[71] Wang, L.X. and Kamath, H., 2006. Modelling hysteretic behaviour in magnetorheological fluids and dampers using phase-transition theory. Smart materials and structures, 15(6), p.1725.

[72] Stanway, R.S.J.L., Sproston, J.L. and Stevens, N.G., 1987. Non-linear modelling of an electro-rheological vibration damper. Journal of Electrostatics, 20(2), pp.167-184.

[73] Yang, G., Spencer Jr, B.F., Carlson, J.D. and Sain, M.K., 2002. Large-scale MR fluid dampers: modeling and dynamic performance considerations. Engineering structures, 24(3), pp.309-323.

[74] Kamath, G.M. and Werely, N.M., 1997. Nonlinear viscoelastic-plastic mechanisms-based model of an electrorheological damper. Journal of Guidance, Control, and Dynamics, 20(6), pp.1125-1132.

[75] Wereley, N.M., Pang, L. and Kamath, G.M., 1998. Idealized hysteresis modeling of electrorheological and magnetorheological dampers. Journal of Intelligent Material Systems and Structures, 9(8), pp.642-649.

[76] Gamota, D.R. and Filisko, F.E., 1991. Dynamic mechanical studies of electrorheological materials: moderate frequencies. Journal of rheology, 35(3), pp.399-425.

[77] Bouc, R., 1971. A mathematical model for hysteresis. Acta Acustica united with Acustica, 24(1), pp.16-25.

[78] Wen, Y.K., 1976. Method for random vibration of hysteretic systems. Journal of the engineering mechanics division, 102(2), pp.249-263.

[79] Ismail, M., Ikhouane, F. and Rodellar, J., 2009. The hysteresis Bouc-Wen model, a survey. Archives of computational methods in engineering, 16(2), pp.161-188.

[80] Spencer Jr, B., Dyke, S.J., Sain, M.K. and Carlson, J., 1997. Phenomenological model for magnetorheological dampers. Journal of engineering mechanics, 123(3), pp.230-238.

[81] Riazi, B., 2021. Design and Investigation of a Semi-Active Suspension System in Automotive Applications (Doctoral dissertation, University of Windsor (Canada)).

[82] Dahl, P.R., 1976. Solid friction damping of mechanical vibrations. AIAA journal, 14(12), pp.1675-1682.

[83] Zhou, Q., Nielsen, S.R. and Qu, W.L., 2006. Semi-active control of three-dimensional vibrations of an inclined sag cable with magnetorheological dampers. Journal of sound and vibration, 296(1-2), pp.1-22.

[84] De Wit, C.C., Olsson, H., Astrom, K.J. and Lischinsky, P., 1995. A new model for control of systems with friction. IEEE Transactions on automatic control, 40(3), pp.419-425.

[85] Lischinsky, P., Canudas-de-Wit, C. and Morel, G., 1999. Friction compensation for an industrial hydraulic robot. IEEE Control Systems Magazine, 19(1), pp.25-32.

[86] Jimnez, R. and Alvarez, L., 2002, December. Real time identification of structures with magnetorheological dampers. In Proceedings of the 41st IEEE Conference on Decision and Control, 2002. (Vol. 1, pp. 1017-1022). IEEE.

[87] Sakai, C., Ohmori, H. and Sano, A., 2003, December. Modeling of MR damper with hysteresis for adaptive vibration control. In 42nd IEEE International Conference on Decision and Control (IEEE Cat. No. 03CH37475) (Vol. 4, pp. 3840-3845). IEEE.

[88] Terasawa, T., Sakai, C., Ohmori, H. and Sano, A., 2004, December. Adaptive identification of MR damper for vibration control. In 2004 43rd IEEE Conference on Decision and Control (CDC)(IEEE Cat. No. 04CH37601) (Vol. 3, pp. 2297-2303). IEEE.

[89] Jiménez, R. and Álvarez-Icaza, L., 2005. LuGre friction model for a magnetorheological damper. Structural Control and Health Monitoring, 12(1), pp.91-116.

[90] Lam, H.F. and Liao, W.H., 2001, August. Semi-active control of automotive suspension systems with magnetorheological dampers. In Smart structures and materials 2001: smart structures and integrated systems (Vol. 4327, pp. 125-136). SPIE.

[91] Wang, D.H. and Liao, W.H., 2004. Modeling and control of magnetorheological fluid dampers using neural networks. Smart materials and structures, 14(1), p.111.

[92] Choi, S.B., Lee, H., Hong, S.R. and Cheong, C., 2000, June. Control and response characteristics of a magnetorheological fluid damper for passenger vehicles. In Smart Structures and Materials 2000: Smart Structures and Integrated Systems (Vol. 3985, pp. 438-443). SPIE.

[93] Ahmadian, M. and Pare, C.A., 2000. A quarter-car experimental analysis of alternative semiactive control methods. Journal of Intelligent Material Systems and Structures, 11(8), pp.604-612.

[94] Metered, H., Bonello, P. and Oyadiji, S.O., 2010. The experimental identification of magnetorheological dampers and evaluation of their controllers. Mechanical systems and signal processing, 24(4), pp.976-994.

[95] Wang, D.H. and Liao, W.H., 2005. Semiactive controllers for magnetorheological fluid dampers. Journal of intelligent material systems and structures, 16(11-12), pp.983-993.

[96] Lai, C.Y. and Liao, W.H., 2002. Vibration control of a suspension system via a magnetorheological fluid damper. Journal of Vibration and Control, 8(4), pp.527-547.

[97] Choi, S.B., Lee, S.K. and Park, Y.P., 2001. A hysteresis model for the field-dependent damping force of a magnetorheological damper. Journal of sound and vibration, 245(2), pp.375-383.

[98] Chang, C.C. and Zhou, L., 2002. Neural network emulation of inverse dynamics for a magnetorheological damper. Journal of Structural Engineering, 128(2), pp.231-239.

[99] Karkoub, M.A. and Zribi, M., 2006. Active/semi-active suspension control using magnetorheological actuators. International journal of systems science, 37(1), pp.35-44.

[100] Dyke, S.J., Spencer Jr, B.F., Sain, M.K. and Carlson, J.D., 1996. Modeling and control of magnetorheological dampers for seismic response reduction. Smart materials and structures, 5(5), p.565.

[101] Metered, H., 2010. Modelling and control of magnetorheological for vehicle suspension systems. The University of Manchester (United Kingdom).

[102] Sims, N.D., Stanway, R., Peel, D.J., Bullough, W.A. and Johnson, A.R., 1999. Controllable viscous damping: an experimental study of an electrorheological long-stroke damper under proportional feedback control. Smart materials and structures, 8(5), p.601.

[103] Du, H., Sze, K.Y. and Lam, J., 2005. Semi-active H∞ control of vehicle suspension with magneto-rheological dampers. Journal of sound and vibration, 283(3-5), pp.981-996.

[104] Metered, H., 2022. Enhancement of Semi-active Vehicle Suspension System Performance Using Magnetorheological Damper (No. 2022-01-5018). SAE Technical Paper.

[105] Guo, D.L., Hu, H.Y. and Yi, J.Q., 2004. Neural network control for a semi-active vehicle suspension with a magnetorheological damper. Journal of Vibration and Control, 10(3), pp.461-471.

[106] Zribi, M. and Karkoub, M., 2004. Robust control of a car suspension system using magnetorheological dampers. Journal of Vibration and Control, 10(4), pp.507-524.

[107] Shen, Y., Golnaraghi, M.F. and Heppler, G.R., 2006. Semi-active vibration control schemes for suspension systems using magnetorheological dampers. Journal of Vibration and Control, 12(1), pp.3-24.

[108] Lam, A.H.F. and Liao, W.H., 2003. Semi-active control of automotive suspension systems with magneto-rheological dampers. International Journal of Vehicle Design, 33(1-3), pp.50-75.

[109] Karnopp, D., Crosby, M.J. and Harwood, R.A., 1974. Vibration control using semi-active force generators.

[110] Bakar, S.A.A., Jamaluddin, H., Rahman, R.A., Samin, P.M. and Hudha, K., 2008. Vehicle ride performance with semi-active suspension system using modified skyhook algorithm and current generator model. International Journal of Vehicle Autonomous Systems, 6(3–4), pp.197-221.

[111] Shojaei, A., Metered, H., Shojaei, S., & Olutunde Oyadiji, S. (2013). Theoretical and Experimental Investigation of Magneto-Rheological Damper based Semi-Active Suspension Systems. International Journal of Vehicle Structures & Systems (IJVSS), 5.

[112] Eshkabilov, S. (2016). Modeling and simulation of non-linear and hysteresis behavior of magneto-rheological dampers in the example of quarter-car model. arXiv preprint arXiv:1609.07588.

[113] Wang, D. H., & Liao, W. H. (2005). Semiactive controllers for magnetorheological fluid dampers. Journal of intelligent material systems and structures, 16(11-12), 983-993.

الخلاصة

تعتبر أنظمة التعليق في المركبات من الأجزاء الأساسية في تطوير صناعة السيارات من خلال زيادة راحة الركوب والموثوقية في القيادة. في هذه الرسالة ، تمت دراسة ومحاكاة نظام التعليق شبه النشط باستخدام تقنية MR damper باستخدام نموذج ربع السيارة في محاكاة استجابة النظام من خلال بيئة Matlab / Simulink. المخمدات المغناطيسية (MR) هي أجهزة تكيفية يمكن تعديل خصائصها من خلال تطبيق إشارة جهد متحكم بها. يجمع نظام التعليق شبه النشط الذي يشتمل على مخمدات MR بين مزايا كل من نظام التعليق النشط والسلبي. لهذا السبب ، كان هناك جهد مستمر لتطوير خوارزميات التحكم لأنظمة تعليق المركبات المثبطة بالرنين المغناطيسي لتلبية متطلبات صناعة السيارات. تهدف هذه الأطروحة إلى التحقيق في التقنيات البارامترية لتحديد الديناميكيات غير الخطية لمثبط MR وتطبيق هذه التقنيات في التحقيق في التحكم في مثبط MR لنظام تعليق السيارة الذي يستخدم الحد الأدنى من المستشعرات ، وبالتالي تقليل تكلفة التنفيذ وزيادة موثوقية النظام. تم اختيار أربعة نماذج بارامترية حديثة ، وتم إجراء مقارنة في محاكاة سلوك مثبط MR. يعتبر السلوك غير الخطي لمثبط MR عقبة أساسية في إجراء محاكاة دقيقة مع أنظمة التحكم التي تم استخدامها ، وهي (Skyhook مع SFM). يعتبر نموذج Bouc-wen المعدل أحد أكثر النماذج دقة في المحاكاة العددية ويعتبر نموذجًا مستقرًا في شرح السلوك الهستيري لمثبط MR. أظهرت النتائج تحسنًا ملحوظًا في تخميد الاهتزازات الناتجة عن شكل الطريق بنسبة 50٪ و 39٪ تقريبًا من الإزاحة الرأسية والتسارع الرأسي مقارنة بالتعليق السلبي.

جمهورية العراق

وزارة التعليم العالي و البحث العلمي

جامعة كربلاء

كلية الهندسة

قسم الهندسه الميكانيكيه

استخدام مخمد مغناطيسي ريولوجي (MR) لتحسين استجابة نظام تعليق السيارة

رسالة مقدمة الى مجلس كلية الهندسة / جامعة كربلاء وهي جزء من متطلبات نيل درجة الماجستير في علوم الهندسة ميكانيك تطبيقي

من قبل:

حسين مهند حسين محي

باشراف :

أ.م.د علي ابراهيم الزغيبي

أ.د عماد قاسم حسين

رجب - 1443   شباط - 2023